

August 5, 2005

To the Graduate School:

This thesis entitled "Using a Spline To Model the Motion Of a 4-man Fireteam During Building Clearing Exercises" and written by Marshall Werner is presented to the Graduate School of Clemson University. I recommend that it be accepted in partial fulfillment of the requirements for the degree of Master of Science with a major in Computer Engineering.

Adam Hoover, Thesis Advisor

We have reviewed this thesis
and recommend its acceptance:

Richard Brooks

Stan Birchfield

Accepted for the Graduate School:

USING A SPLINE TO MODEL THE MOTION OF A
4-MAN FIRETEAM DURING BUILDING CLEARING
EXERCISES

A Thesis
Presented to
the Graduate School of
Clemson University

In Partial Fulfillment
of the Requirements for the Degree
Master of Science
Computer Engineering

by
Marshall Werner
August 2006

Advisor: Dr. Adam Hoover

ABSTRACT

This paper examines the problem of tracking positions of a fireteam (4-5 men) as they perform building clearing exercises in order to predict future motion of the team. This was done by examining the team as a single entity rather than 4 or 5 separate entities. A team model was used under the assumption that the team stays together as a group and moves in specific patterns. The model chosen for this experiment was a spline curve. This spline curve allowed for movement in straight lines through hallways as well as curving around corners.

Two experiments were conducted to help predict the future motion of the team. The first experiment extended the curve created by the current team member positions. Five different extensions were examined: a straight line extension, a straight line extension from the tangent formed at the last team member, a curve in which the curvature of the spline remained the same through the extension, a curve in which the curvature dissipates through the extension, and a curve in which the curvature increases through the extension. The distance of the team from the predicted line was measured. The second experiment performed measured how well the team retained their configuration as they moved. This was done by taking the area difference between the spline created at the current location and the spline at future locations.

The results of the experiment show that applying a geometric model to the team and examining their movement as a whole instead of separate entities can be useful in predicting the future positions of the team members. In a hallway, extending the curve does well for predicting time into the future, 1.75 seconds, but not as well for distance, only 20 cm. The configuration of the team remains relatively constant since they are moving in a line. As for entering the room, the extension methods do well for distance, 32 cm, but only 0.3 seconds. This means that team does a good job of playing “follow-the-leader” into the

room. The configuration changes due to the quick acceleration of the team, however it is mainly caused by a “stretching” of the team configuration. For the room data the prediction method for movement is minimal, 18 cm and 0.2 seconds, due to the fact that they spread out to cover the entire room. This also causes a large change in configuration. Overall, the spline model shows merit in predicting the team’s future positions as they enter the room, however, the experiments show that this model warrants further development.

TABLE OF CONTENTS

	Page
TITLE PAGE	i
ABSTRACT	ii
LIST OF TABLES	v
LIST OF FIGURES	vi
1 Introduction	1
1.1 Background	1
1.2 MOUT Background	6
2 Methods	12
2.1 Spline Overview	12
2.1.1 Method Used To Develop Spline	17
2.2 Spline Extension	18
2.3 Configuration Retention	22
2.4 Data	24
3 Results	26
3.1 Spline Extension Prediction Results	26
3.2 Configuration Retention Results	41
4 Conclusions	47
BIBLIOGRAPHY	50
APPENDICES	53
A Entire Extension Graphs	53

LIST OF TABLES

Table	Page
2.1 Comparison of seven different types of splines [15].	15
3.1 Results of the position prediction experiment.	40

LIST OF FIGURES

Figure	Page
1.1	Images showing independent and dependent team motion. 3
1.2	A CAD view of the shoothouse and instructor station. 7
1.3	An image of the camera network at the shoothouse. 8
1.4	Equipment used in building clearing exercises. 9
1.5	Playback tool used for review and cleaning shoothouse data. 10
1.6	Images showing raw data of fireteam movement into the first room. 11
1.7	Images showing clean data of fireteam movement into the first room. 11
2.1	A generic image of a spline. 13
2.2	A view of the various extension curves used to predict future motion. 20
2.3	A plot showing the area between two splines at various sampling resolutions. 24
2.4	A 2-dimensional view of the shoothouse. 25
3.1	Frame extension results for trial 1 hall data. 27
3.2	Distance traveled extension results for trial 1 hall data. 28
3.3	Frame extension results for trial 1 entering room data. 29
3.4	Distance traveled extension results for trial 1 entering room data. 30
3.5	Frame extension results for trial 1 room data. 31
3.6	Distance traveled extension results for trial 1 room data. 32
3.7	Total data points for each distance in the trial 1 room entering data file. . . . 33
3.8	Average distance from curve for time in future for hall data. 34
3.9	Average distance from curve for team distance traveled in future for hall data. 35
3.10	Average distance from curve for time in future for entering data. 36

3.11	Average distance from curve for team distance traveled in future for entering data.	37
3.12	Average distance from curve for time in future for room data.	38
3.13	Average distance from curve for team distance traveled in future for room data.	39
3.14	Average area between configurations based on time.	42
3.15	Average area between configurations based on average distance traveled. . .	43
3.16	Example of a 0.17 m ² change in configuration.	44
3.17	Example of a 1 m ² change in configuration.	45
3.18	Example of a 5 m ² change in configuration.	46
A.1	Entire average distance from curve by frames graph for hall data.	53
A.2	Entire average distance from curve by distance graph for hall data.	54
A.3	Entire average distance from curve by frames graph for room entering data.	55
A.4	Entire average distance from curve by distance graph for room entering data.	56
A.5	Entire average distance from curve by frames graph for room data.	57
A.6	Entire average distance from curve by distance graph for room data.	58

Chapter 1

Introduction

1.1 Background

This research examines the problem of tracking the positions of members of a fireteam (4-5 members) as they perform a building clearing exercise. A fireteam is defined as four or five team members working together as a group in order to perform the building clearing exercises. Position tracking is accomplished using a network of video cameras, installed throughout the building, similar to a video surveillance network. We are interested in the two-dimensional floor-plane coordinates of each member of the fireteam, on the accuracy of 5-10 cm. The building clearing exercise involves the fireteam moving room to room, in general, moving as a cohesive unit, engaging enemies and identifying non-combatants. This thesis considers how to track the fireteam as one entity rather than as 4-5 independently tracked people.

Tracking data from a fireteam has many potential uses. The data can be replayed for after-action review in order to train and to improve the team's ability to clear the building properly. This data can also be used to develop databases of expert versus novice fireteams in order to analyze training trends and improve practices. Along with improving training, the data can be used to improve building clearing techniques used in practice. More specific

to our particular research project, which will be discussed in more detail in Section 1.2, it can improve the tracking inside the shoothouse which will ultimately lead to improve the cleaning process by reducing time and man-power spent cleaning each raw data file.

As well as helping to improve the offensive techniques, fireteam tracking can also be used on the defensive side. Tracking data can be used to develop simulated AI enemies in virtual reality simulations based upon real expert recordings. This will allow for new defensive techniques to be developed. Also having databases of team movement could allow fireteams to predict enemy movement and adjust accordingly.

There are several different types of floor-plane position tracking technologies currently being developed, including GPS, camera networks, floor mats, LED-light based tracking, and RFIDs. However, none of the technologies are able to track a group of people at the needed update rate (20-30 Hz to capture running motions) and the needed accuracy (5-10 cm to capture room-position level of detail). The best technology available is a camera network, which fails due to various lighting conditions and shadows as well as when team members are in close proximity to each other. Our goal is to improve the camera network tracking under the assumption that a fireteam stays together and moves in specific patterns. Specifically we try to model the team motion using a spline. Before explaining the spline model, we look at some of the related literature in which other groups (objects or people) have been tracked as a team.

Before explaining current work being done with team tracking, it necessary to explain what is meant by team tracking. Figure 1.1 shows how team members can move (a) independently or (b) dependently of the other team members¹. There are several different types of team tracking used depending on the interaction of the team as well as the action being performed by the team.

The first area of research being used for team tracking uses a team of sensors. Much of this research has involved tracking a team of objects Localized scale(usually robots) as sep-

¹The term move is used to simplify the explanation, however, the independent or dependent team interaction can refer to any action performed by the team.

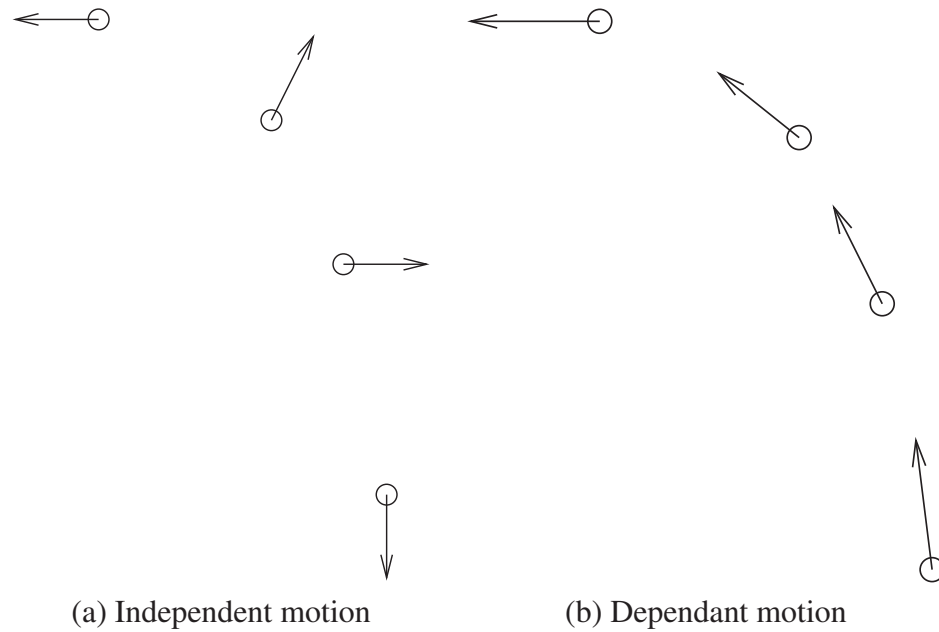


Figure 1.1: Images showing independent and dependent team motion.

arate entities. One approach tracks various objects that are working independently of each other to accomplish a goal. In one study, teams of autonomous robots are used to develop a map of an unknown terrain and orient themselves based on the map and the other robots' positions in relation to the newly developed map [12]. A second study uses autonomous mobile robots to track a target and avoid obstacles. This is done using ultrasonic and vision sensors [9]. This research is being expanded by trying to optimize the search algorithm to improve target tracking [22]. Although there is very little research in the field of geometrically tracking a team consisting of human members, there is some research in pedestrian tracking. Groups of humans have been tracked crossing a street [17]. This is done using several computer vision techniques in order to improve safety at crosswalks. Although the pedestrians can cause other pedestrians to change course, the tracking is individually based, and the pedestrians are not controlled by an outside system. In all of these studies there is a group of sensors tracking the objects as they move independently of each other.

The second area of research uses a single station to control the motion of the team. One such study consists of a team of satellites orbiting the earth, communicating with each

other and ground base stations, in order to monitor fires and volcanoes [11]. On a more localized scale, host robots (leaders) are used to distribute various small tasks to a team of worker robots in order to accomplish a larger goal [26]. Currently, the biggest area of research for teams of robots in which the team is commonly controlled is games. The biggest robot game being researched and developed is RoboCup. Many researchers have worked on RoboCup teams [5, 24, 20, 19]. These robots work as a team to play soccer. This has developed into a very popular area of research and groups all over the world are designing teams to compete against each other [24]. The popularity of RoboCup has led to other games. One such game is capture-the-flag. This is played using a limited human commander and a UAV for position data. The commander and UAV communicate with the team of robots in order to compete in a game of capture-the-flag [4]. Even though all of the team members are commonly controlled, the tracking of the team is still individually based.

The third area of research is modeling team motion. This research tracks objects as they work together as a team. With the development of high speed cameras, the dispersion of particles is tracked in a turbulent flow in order to compare the results to theoretical predictions [8]. Although the motion seems to be random and independent, it is caused by the existence of other particles. Another area of research for team modeling is tracking teams through building clearing exercises, the current project being discussed. In this study teams are tracked as a single entity they move together throughout the shoothouse.

The final area of research tracks teams as they perform tasks other than movement. Even though there is a lack of research in physical tracking of human teams, there is much research using human teams in other domains. One such area is document editing and coding. This research studies team performance where team members communicate remotely versus when they are all in the same room to complete a task [23]. Another study uses competition and rewards to improve team skills. Team members are rewarded for task completion, which increases as team involvement increases [10]. There is also a lot

of research in improving teamwork skills in college students. One approach gives questionnaires to the team members so that the team can adjust to the responses in order to improve [2]. Another approach is to provide external leadership to the team (usually a graduate student). The mentor helps build team confidence and trust which increases teamwork and productivity [13]. A third approach develops a project that simulates industry as much as possible. This allows the students to develop teamwork skills by working as they would in industry [7].

To our knowledge, we are the first research team to look at tracking the physical positions of a group of people using a team model. For our research, we chose to model the team using a spline. The idea is, that in certain circumstances, the team plays “follow the leader”. For example, when the team stacks in the hallway against a wall and move in a line along the wall and around corners to advance. Also as the team bursts into a room, they start from a stacked position in the hallway and follow the lead man of the fireteam into the room to clear the room or engage in combat if needed. The team tends to move like a train, following the track that the leader (team member in the front) lays out. A spline was chosen because it will fit a curve to the initial positions and will allow for curvature that straight line interpolation will not. Therefore, this seems like a more natural way to predict team motion along the track and to maintain the team configuration.

The following section gives an overview of MOUT and the design of our test facility and equipment. An overview of splines can be found in Section 2.1. Using this model, two studies were performed. The first study extends the spline in order to predict future movement of the team. This process can be found in Section 2.2. The second study, shown in Section 2.3, measures how well the team retains the same configuration. The results of the two studies can be found in Chapter 3.

1.2 MOUT Background

In this section we provide some background on the importance of MOUT, or military operations in urban terrain. We also describe the training facility built to record the building clearing exercises, including the technical details of the video camera network tracking system.

In recent years, the US military has shifted its military operations from the historic battlefield fighting to urban combat. This can be seen in recent conflicts such as Somalia, Kosovo, Afghanistan, and most recently, Iraq. The increase in urban combat has shifted the focus of military research toward MOUT techniques. The issues of fighting in a city have only recently been addressed in US Army doctrine (manuals and other official training documentation) [14, 1]. Currently, U.S. marines are deployed with approximately one week of training in MOUT, with essentially no objective evaluation or testing of that training. North Atlantic Treaty Organization (NATO) and Partners for Peace (PfP) countries look to the U.S. for leadership in developing MOUT procedures and training [6].

MOUT training research and development is still very young. Currently live training involves soldiers learning techniques in mock buildings or towns. The US Marine base in Quantico, Maryland is currently equipped with two concrete block towns. Here, a training officer shows the soldiers positioning and movement, and the soldiers perform mock exercises. A few bases have installed cameras and microphones to record the exercises for after-action review. The U.S. Army base at Fort Polk, Louisiana, was the first to be so equipped [16]. These facilities typically run platoon sized operations, (approximately 40 men) with limited tracking accuracy (1 m) and update rate (1 Hz).

Our research facility is a zoomed in version of one of these towns. We currently have a single building and train using a fireteam of 4-5 men. The facility is located at the 263rd Army National Guard Air and Missile Defense Command site in Anderson, SC. This site was chosen due to its proximity to Clemson University. It is a large warehouse so there is a large open area that has been made available to us for our building, which covers

approximately 200 m². This facility also gives us access to ready and willing volunteers, including the 400 active personnel and the Clemson ROTC who practice there. The training facility consists of two parts, a shoothouse and an instructor station. The instructor station is the area in which all of the data is collected, recorded, and processed. It also has an area in which the fire team can review the data after a run is completed. The shoothouse is the area in which the live building clearing exercises are performed and recorded. The shoothouse consists of six rooms and interconnecting hallways. The rooms can be reconfigured to vary the size, shape, or entry point. Figure 1.2 shows a CAD view of the shoothouse and the instructor station.

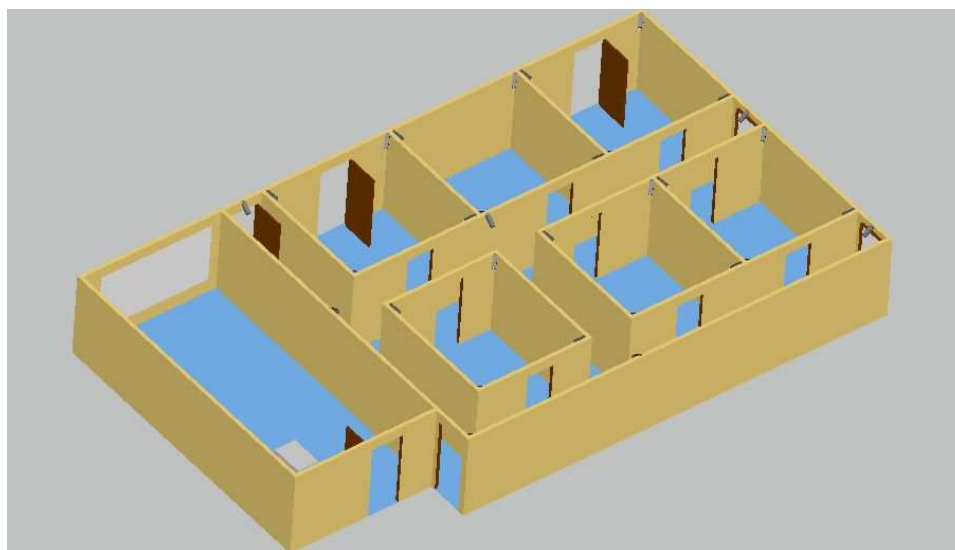


Figure 1.2: A CAD view of the shoothouse and instructor station.

The shoothouse is installed with thirty-six cameras positioned for tracking the position of trainees throughout the shoothouse during building clearing exercises. These cameras are wired to a rack of computers which record the video and process it in real-time to track the floor- plane geometric coordinates of the fireteam. These tracks are updated at a rate of 20 frames per second and are accurate to within approximately 10 cm. Figure 1.3 shows an image of the camera network installed at the shoothouse. The camera network is set up so that there are six cameras associated with each room. Four cameras are placed in the corners of each room looking into the room. The other two cameras are placed at the

corners of the room adjacent to the interconnecting hallway facing into the hallway. This gives each room four cameras to track action and each section interconnecting hallway² between two rooms four cameras. This network is designed to record action and track positions anywhere in the shoothouse.



Figure 1.3: An image of the camera network at the shoothouse.

Along with position tracking at the shoothouse, we have built weapons and helmets that work similar to laser tag equipment. This equipment uses infrared to simulate shots fired and hits detected. This equipment also detects orientation, so that the direction of the rifle and the direction that the team member is facing can be recorded. Figure 1.4 shows the equipment used in our shoothouse for building clearing exercises. The rifle can be seen in Figure 1.4(a) and the helmet in Figure 1.4(b). For more information about the design of this equipment please refer to the paper by Waller [25]. There is also a device that is worn by the fireteam referred to as a Wearable Arousal Meter (WAM). This device measures heart

²Some of the hallways are not used during the building clearing exercises. The hallways used are the one seen in figure 1.2 that separates the shoothouse from the instructor station and the one between the rooms. These are the hallways that are referred to as interconnecting hallways.

rate activity. The WAM can be seen in Figure 1.4(c). To find more information about the WAMs, refer to the papers by Hoover and Muth [18, 21].

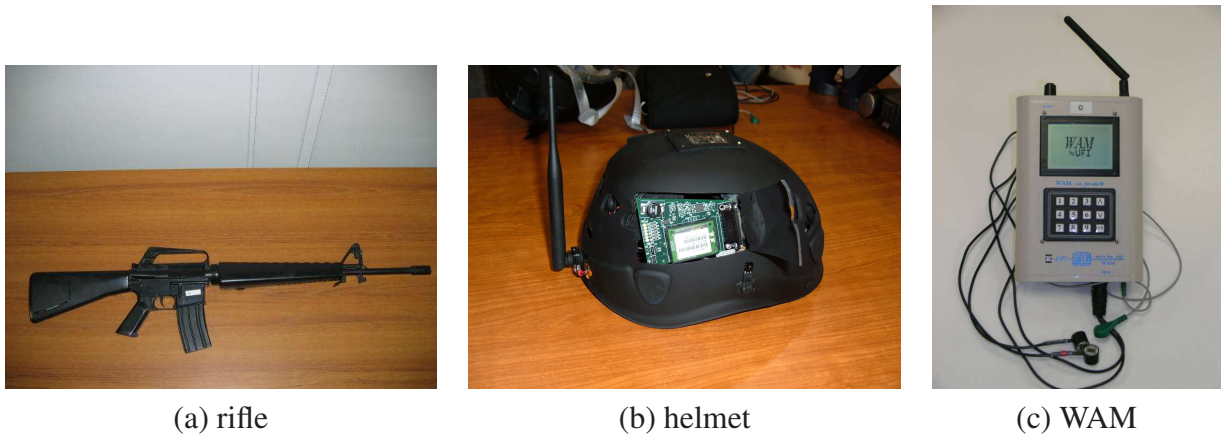


Figure 1.4: Equipment used in building clearing exercises.

In order to view the data that is recorded from the equipment and the cameras and to clean the data, we developed a playback tool. Figure 1.5 shows the playback tool designed by our research team. The white lines outline the wall of the shoothouse. The four circles to the bottom right of the shoothouse symbolize the fireteam. The other circles throughout the shoothouse symbolize combatants and non-combatants. The arrows in the bottom left are the buttons to advance and rewind frames. The image in the top right is the current frame at the selected camera. The items under the image show the rifle data (labeled R), helmet data (labeled H) and WAM data (labeled W) matched to the appropriate person by color.

This playback tool can be used to view the raw data collected from the exercises. An example of a few frames of raw data of the team moving through the hallway and entering the room can be seen in Figure 1.6. This is a section of the shoothouse that shows the initial movements of the team as they enter the first room. The three images show the raw data for the fireteam at time frame 0 (0 seconds), 300 (15 seconds), and 360 (18 seconds).

As can be seen in Figure 1.6 the tracking system does not work nearly as well as needed for position tracking. Once the raw data is collected, someone has to go through each raw

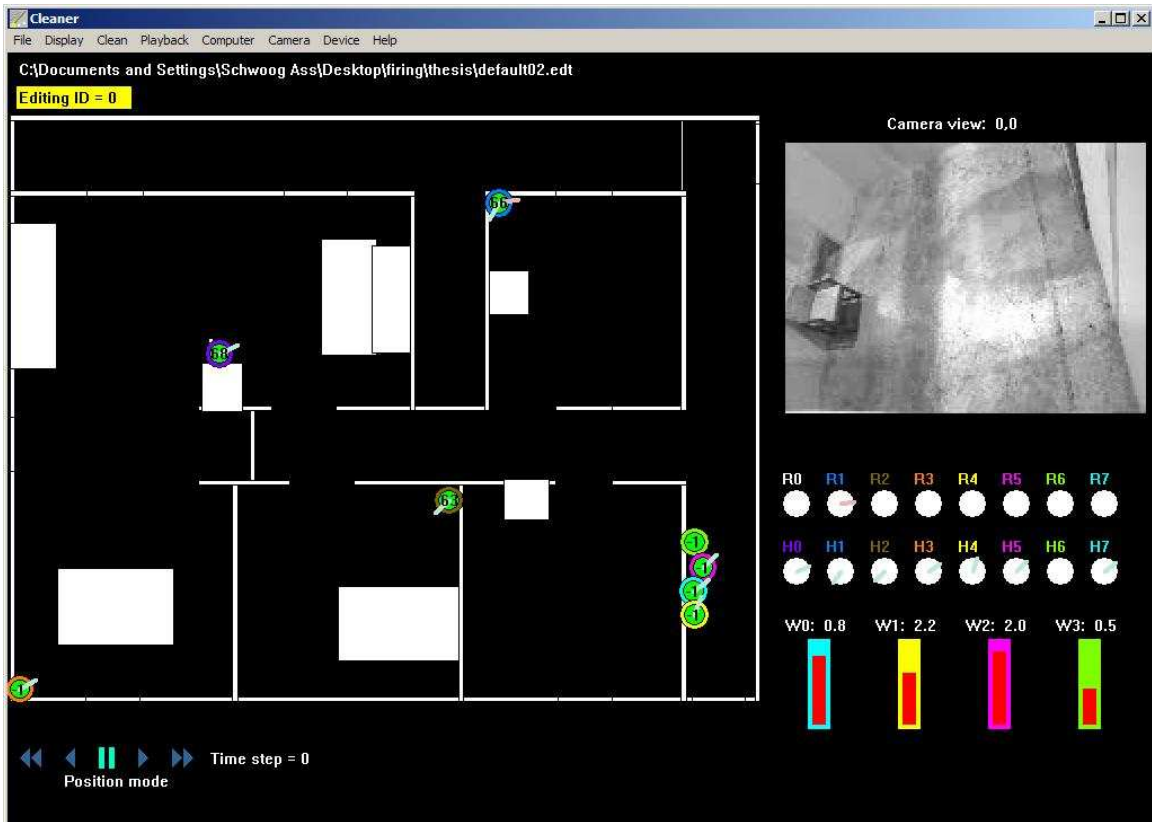


Figure 1.5: Playback tool used for review and cleaning shoothouse data.

data file manually and clean the data. This cleaning process consists of adding data points where needed and adjusting the current data tracks, so that they are in the proper location. Figure 1.7 shows the cleaned fireteam positions for the same three frames. This is a very tedious and time consuming process. This cleaning process is what led to a desire to be able to predict future motion to ultimately lead to a better position tracker.

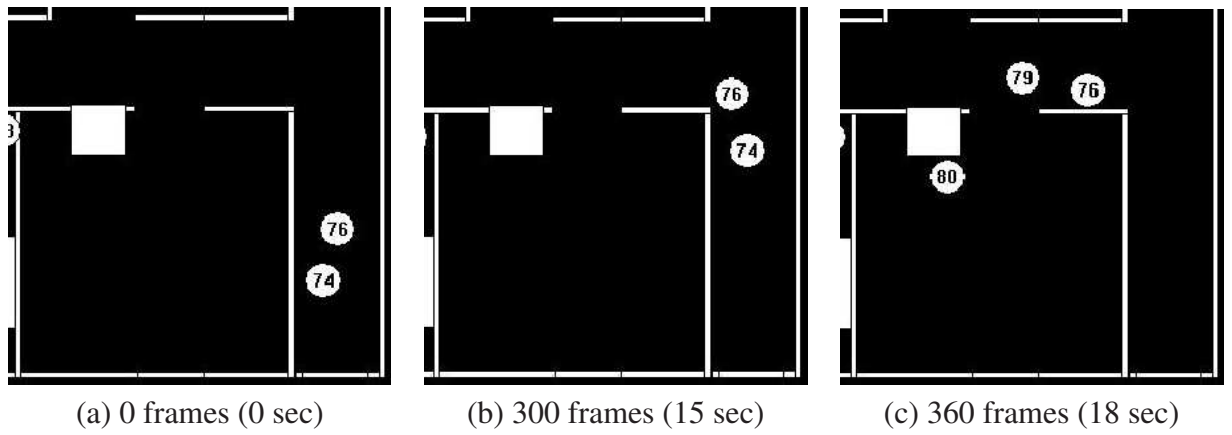


Figure 1.6: Images showing raw data of fireteam movement into the first room.

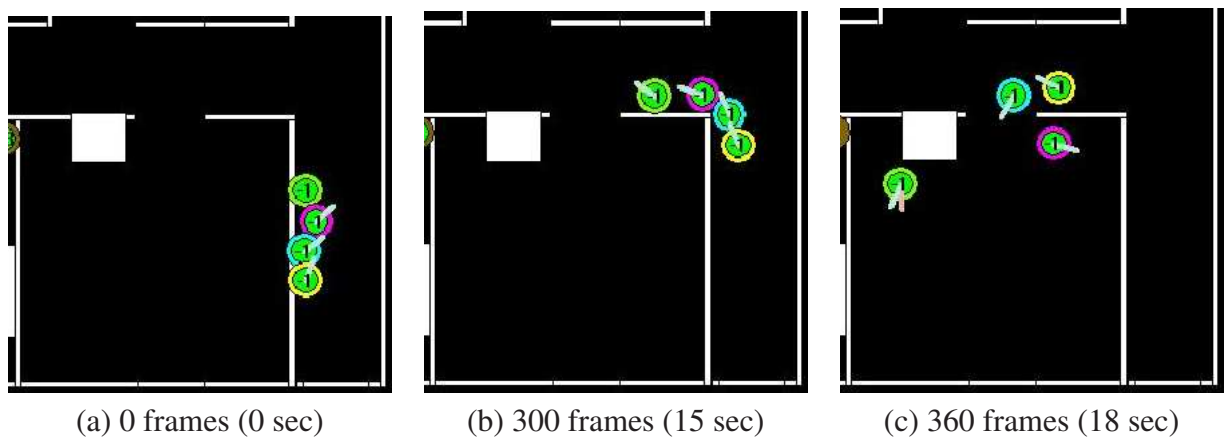


Figure 1.7: Images showing clean data of fireteam movement into the first room.

Chapter 2

Methods

2.1 Spline Overview

This section will give a general introduction to splines and the techniques used in our research. The specific details of our approach will be discussed in the following two sections. Spline functions are commonly used in computer aided design and computer graphics. They are generally used to interpolate curves that do not have a physical mathematical model. Splines are used to generate complex shapes and movements to add a smoothness to an otherwise jittery interpolation. Splines are used over other types of interpolation due to the closeness of their results to other results and their simplicity and accuracy [27].

A spline is defined as a piecewise function where each piece is defined by a polynomial. Typically these polynomial pieces consist of parametric equations in which t is defined on the interval $[0,1]$. The order of the polynomial can be any value, however, a cubic polynomial is usually chosen. Cubic polynomials usually give the accuracy needed for the curve while keeping the calculations to a minimum. Known control points are used to define the polynomial curves. The number of control points needed for each piece depends on the type of spline used. Along with the control points, some types of splines require

knowledge of the tangents at the control points. Figure 2.1 shows a generic spline curve with the control points and a tangent at one of the control points labeled.

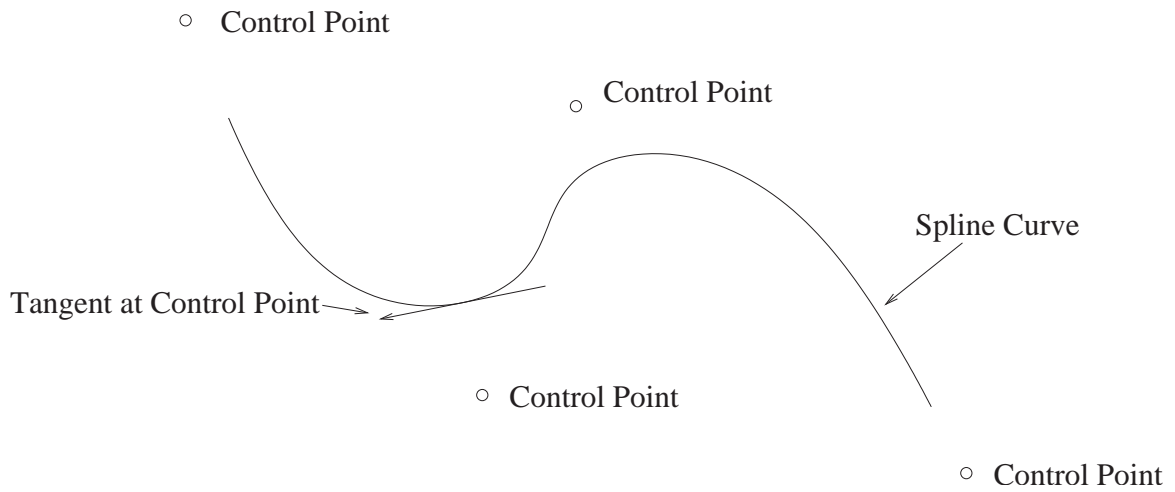


Figure 2.1: A generic image of a spline.

The general equation for each piece of a spline along the given interval of t is defined as

$$Q(t) = T \times M \times G \quad (2.1)$$

where $Q(t)$ is the coordinate point of the spline at time t , T is a 1×4 matrix of the polynomial parameters, M is a 4×4 basis matrix and G is a 4×2 geometric matrix (G can be adjusted according to the dimensions of the coordinate system). The expanded equation for $Q(t)$ can be seen in Equation 2.2.

$$Q(t) = \begin{bmatrix} t^3 & t^2 & t & 1 \end{bmatrix} \begin{bmatrix} m_{11} & m_{12} & m_{13} & m_{14} \\ m_{21} & m_{22} & m_{23} & m_{24} \\ m_{31} & m_{32} & m_{33} & m_{34} \\ m_{41} & m_{42} & m_{43} & m_{44} \end{bmatrix} \begin{bmatrix} G_{1x} & G_{1y} \\ G_{2x} & G_{2y} \\ G_{3x} & G_{3y} \\ G_{4x} & G_{4y} \end{bmatrix} \quad (2.2)$$

Although the above equation applies to splines in general, the values used can vary greatly. The values used are dependent on the constraints on the spline, the information known about the spline, and the specific application for the spline¹. Table 2.1 shows seven of the most commonly used types of splines (listed in bold across the top) and several of the most important properties that are used to choose a particular spline (listed down the left hand side) [15].

The first property is whether or not the convex hull is defined by the control points. The convex hull is defined as the minimal convex set containing all of the points. This means that this is the smallest area polygon created by connecting points with straight lines within which all of the points are contained. To visualize this in 2-dimensions, imagine stretching a rubber band around all of the points and releasing it. The shape formed by the rubber band would represent the convex hull. For 3-dimensions, imagine using a balloon instead of a rubber band.

The next two properties involve the number of control points used in the interpolation of the spline. All splines are developed using the control points. However, some of the splines do not use any of the control points in their interpolation, similar to a best fit curve. Other splines use some of the control points in the interpolation. Usually this means that the endpoints of each of the piecewise functions are control points, but the spline can be generated to use any number. There are also some splines that require all of the control points be used in the interpolation.

The next property is the ease of subdivision. Subdividing involves adding control points to a segment of the spline to reach a desired result that may not be reached with the current number of control points. The ease of the subdivision refers to the adjustments that must be made to the calculations in order to reach the desired effect using existing data.

The fifth and sixth properties deal with continuities. The first shows which continuities are inherent in the representation of the spline while the second shows which continu-

¹Many splines are application specific and lead to adjustments made to values of the general M basis matrix of a particular type of spline.

	Hermite	Bézier	Uniform B-spline	Uniformly Shaped β -spline	Nonuniform B-spline	Catmull-Rom	Kochanek-Bartels
Convex hull defined by control points	N/A	Yes	Yes	Yes	Yes	No	No
Interpolates some control points	Yes	Yes	No	No	No	Yes	Yes
Interpolates all control points	Yes	No	No	No	No	Yes	Yes
Ease of subdivision	Good	Best	Avg	Avg	High	Avg	Avg
Continuities inherent in representation	$C^0 G^0$	$C^0 G^0$	$C^2 G^2$	$C^0 G^2$	$C^2 G^2$	$C^1 G^1$	$C^1 G^1$
Continuities easily achieved	$C^1 G^1$	$C^1 G^1$	$C^2 G^2$	$C^1 G^2$	$C^2 G^2$	$C^1 G^1$	$C^1 G^1$
Number of parameters controlling a curve segment	4	4	4	6	5	4	7

Table 2.1: Comparison of seven different types of splines [15].

ities are easily achieved, which “refers to constraints such as forcing control points to be collinear to allow G^1 continuity” [15]. The two types of continuity are geometric continuity (G) and parametric continuity (C). The geometric continuity G^0 simply means that two curve segments join, G^1 means that the tangents of the two curves are equal at the joint. Parametric continuity is similar to this, except that the two curves are parametric curves and the continuities occur at the segments’ joint points. C^n continuity occurs if direction and magnitude are equal at joint point for $d^n/dt^n[Q(t)]$ through the n th derivative [15] where

$$Q(t) = [x(t) \ y(t) \ z(t)] \quad (2.3)$$

and

$$\begin{aligned} x(t) &= a_x t^3 + b_x t^2 + c_x t + d_x \\ y(t) &= a_y t^3 + b_y t^2 + c_y t + d_y \\ z(t) &= a_z t^3 + b_z t^2 + c_z t + d_z \quad 0 \leq t \leq 1 \end{aligned} \quad (2.4)$$

The final property is the number of parameters controlling a curve segment. These values include the 4 geometric values, i.e) control points and/or tangents needed, as well as any other values that may be needed, such as parameters used in tangent calculations.

In our particular case, the most important property is that the spline interpolates all of the control points. According to the table, there are three choices that follow this criterion, the Hermite curve, the Catmull-Rom curve and the Kochanek-Bartels curve. These three curves are really all the same curve. The basis matrix is the same for all three and the geometric matrix requires the same information, two control points and the tangent at those points to develop a curve. Excluding the continuities mentioned in the chart, the only difference between the Hermite and the other curves is that the Hermite curve uses *a priori*

knowledge of the tangents and the others calculate tangents based on the surrounding control points. The Kochanek-Bartels curve is similar to the Catmull-Rom curve except that it adds three parameters, tension, bias, and continuity, to the calculation of the tangent². The Catmull-Rom is a Kochanek-Bartels curve in which the three parameters are zero. Because we did not have *a priori* knowledge of the tangents the more general form was chosen. After testing various parameters, it was decided that setting them to zero and choosing the simplified form or the Catmull-Rom curve was the best choice.

2.1.1 Method Used To Develop Spline

Before discussing the various methods for extending the spline, an explanation of the spline used is needed. Using the known locations of the the control points, $p_0 \dots p_n$, the x and y coordinates of the tangent vector, θ_{i_x} and θ_{i_y} respectively, are found using Equations 2.5 for $i = 0 \dots n$. The endpoints are repeated such that $p_0 = p_{-1}$ and $p_n = p_{n+1}$. The angle of the tangent θ_i can be found using Equation 2.6. Using Equations 2.5 and Equation 2.6 the tangents are reduced to the straight line tangents between the endpoint and the first interior control point. Therefore the equation set must be adjusted to better define a tangent for the curve. Equations 2.7 and 2.8 were developed and used to better define the initial and final endpoint tangents respectively.

$$\begin{aligned}\theta_{i_x} &= \frac{1}{2}(x_i - x_{i-1}) + \frac{1}{2}(x_{i+1} - x_i) \\ \theta_{i_y} &= \frac{1}{2}(y_i - y_{i-1}) + \frac{1}{2}(y_{i+1} - y_i)\end{aligned}\tag{2.5}$$

$$\theta_i = \arctan\left(\frac{\theta_{i_y}}{\theta_{i_x}}\right)\tag{2.6}$$

²Kochanek-Bartels are also known as TCB splines due to the parameters tension, bias, and continuity.

$$\begin{aligned}\theta_{0_x} &= \cos(2\theta_0 - \theta_1) \\ \theta_{0_y} &= \sin(2\theta_0 - \theta_1)\end{aligned}\tag{2.7}$$

$$\begin{aligned}\theta_{n_x} &= \cos(2\theta_n - \theta_{n-1}) \\ \theta_{n_y} &= \sin(2\theta_n - \theta_{n-1})\end{aligned}\tag{2.8}$$

Using the general equation for a spline, Equation 2.2, and the basis matrix M from Equation 2.9, the equation for the points along the spline, $Q_i(t)$ for $i = 0 \dots n - 1$ and t on the interval $[0,1]$, can be seen in 2.10.

$$M = \begin{bmatrix} 2 & -2 & 1 & 1 \\ -3 & 3 & -2 & -1 \\ 0 & 0 & 1 & 0 \\ 1 & 0 & 0 & 0 \end{bmatrix}\tag{2.9}$$

$$Q_i(t) = \begin{bmatrix} t^3 & t^2 & t & 1 \end{bmatrix} \begin{bmatrix} 2 & -2 & 1 & 1 \\ -3 & 3 & -2 & -1 \\ 0 & 0 & 1 & 0 \\ 1 & 0 & 0 & 0 \end{bmatrix} \begin{bmatrix} x_i & y_i \\ x_{i+1} & y_{i+1} \\ \theta_{i_x} & \theta_{i_y} \\ \theta_{(i+1)_x} & \theta_{(i+1)_y} \end{bmatrix}\tag{2.10}$$

2.2 Spline Extension

We seek to determine if we can predict future position of the fireteam by using the current positions and the spline developed to model the team. This is done by extending the

spline developed for the four known positions. The extensions will be done in five different approaches. The following section details each approach.

The first step was to develop a control curve. This curve used simple straight line connection between the control points. In order to extend this curve, new control points are needed. Assuming that the 4 known control points of the fireteam are labeled p_0 , p_1 , p_2 , and p_3 , the extended control points p_4 , p_5 ... are found using Equations 2.11, 2.12, and 2.13. The distance between the new control point and the previous point is equivalent to the distance between points p_2 and p_3 in the same direction as from p_2 to p_3 .

$$d_i = \sqrt{(x_{i-1} - x_{i-2})^2 + (y_{i-1} - y_{i-2})^2} \quad (2.11)$$

$$\theta_{i-1,i} = \arctan\left(\frac{y_i - y_{i-1}}{x_i - x_{i-1}}\right) \quad (2.12)$$

$$\begin{aligned} x_i &= x_{i-1} + d_i \cos(\theta_{i-1}) \\ y_i &= y_{i-1} + d_i \sin(\theta_{i-1}) \end{aligned} \quad (2.13)$$

In order to predict future positions of the team extra control points need to be added to extend the spline created for the four known positions. Several different extension methods were tested. Figure 2.14 shows the different extension methods that were tested. Curve A is the straight line control curve. Curve B extends the tangent formed at the endpoint of the spline in a straight line. Curve D keeps the same curvature of the last section of the spline for the four known positions and continues that curvature. Curve C uses the last section but slowly dissipates the curvature. Curve E also uses the last section of the spline but slowly increases the curvature.

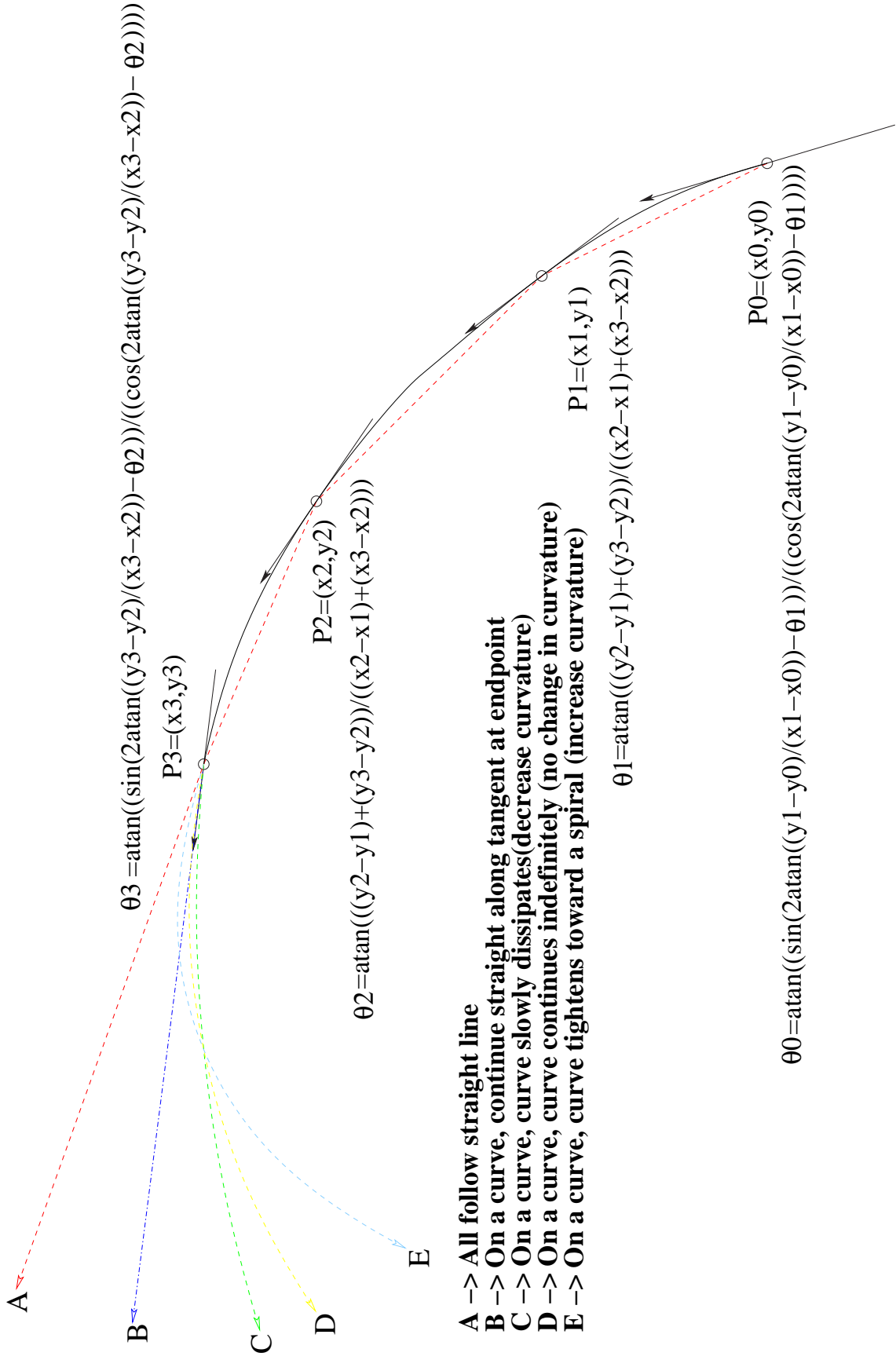


Figure 2.2: A view of the various extension curves used to predict future motion.

The first extension is a straight line extension along the tangent at p_3 . The tangent angle, θ_3 , is found using Equations 2.8 where $n = 3$ and Equation 2.6. Using the formulas from Equations 2.11 and 2.13 as well as θ_3 , the first extension point, p_4 can be found. This process is repeated for p_5 and all subsequent extension points except that the tangents are found using Equation 2.12.

The next extension method is to extend the spline with the same curvature as the last section of the spline created by the known fireteam positions. To find an extended control point, p_i for $i = 4 \dots n$ the tangent θ_{i-1} for p_{i-1} is found using Equations 2.5, 2.8, and 2.6. Next, θ_{i-2} for p_{i-2} is found using Equations 2.5 and 2.6. The straight line tangent, $\theta_{i-2,i-1}$ is also found between p_{i-1} and p_{i-2} using Equation 2.12. Once these three θ values are found, the coordinates for the new control point can be found using Equations 2.14.

$$\begin{aligned} x_i &= x_{i-1} + d_i \cos(\theta_{i-2,i-1} + (\theta_{i-1} - \theta_{i-2})) \\ y_i &= y_{i-1} + d_i \sin(\theta_{i-2,i-1} + (\theta_{i-1} - \theta_{i-2})) \end{aligned} \quad (2.14)$$

The other two extension methods, curve extension with dissipating and increasing curvature follow the same procedure as mentioned above for the curve extension, except that the coordinate equations vary as shown in Equations 2.15 and 2.16 respectively, where p is the number of known control points (4 in our case).

$$\begin{aligned} x_i &= x_{i-1} + d_i \cos(\theta_{i-2,i-1} + \frac{1}{2^{i-p}}(\theta_{i-1} - \theta_{i-2})) \\ y_i &= y_{i-1} + d_i \sin(\theta_{i-2,i-1} + \frac{1}{2^{i-p}}(\theta_{i-1} - \theta_{i-2})) \end{aligned} \quad (2.15)$$

$$\begin{aligned} x_i &= x_{i-1} + d_i \cos(\theta_{i-2,i-1} + 1.3^{i-p}(\theta_{i-1} - \theta_{i-2})) \\ y_i &= y_{i-1} + d_i \sin(\theta_{i-2,i-1} + 1.3^{i-p}(\theta_{i-1} - \theta_{i-2})) \end{aligned} \quad (2.16)$$

In the above mentioned extensions, all of the control points are found before a spline is fit to them, with the exception of the tangent straight line extension. For this curve, the spline is fit to the known control points and then the tangent is extended in a straight line. However, this spline fitting after finding all of the control points can cause a small variation in the tangents of the extended points. This variation is minimal and the error that it causes is negligible to our results due to the limited number of control points added and the limited distance traveled by the fireteam.

These extensions were tested at various times and distances in the future. This was done to see how far into the future we could predict the team's positions. Time into the future was done every 5 frames, or 0.25 seconds. The distance into the future measurements were taken for every frame but sorted by the average distance that the team moved. These values were averaged for each time and distance over all of the trials for each data set. Results can be seen in Section 3.1 for the extension prediction experiment.

2.3 Configuration Retention

The next study was to test how well the team retained their configuration. This test was done similarly to the previous test, by testing at certain time steps and distances in the future. For the time test, a spline was developed every five frames, or 0.25 seconds, using the four known positions of the team. This spline was traversed and using the distance formula from Equation 2.11, the total distance of the spline was found. This total distance was divided by the number of points on the spline, N , in order to get a width, w , of each interval of t . Then for each subsequent five frames, a spline was developed for those four fireteam positions. The centroid for each of the splines was found using Equations 2.17. The centroids were subtracted from each point on the appropriate spline, so that the splines were centered about the origin. Then the distance between the two points of each spline for every value of t were found and multiplied by the width, w . This value was summed to

get a total area between the two curves. Equation 2.18 shows the formula used to find the area. This area was averaged for future time steps similarly to the extension method. This test was also repeated using average distance traveled by the team similar to the extension method. The results for the two tests were averaged over all ten trials and can be seen in Section 3.2.

$$\begin{aligned}\bar{x} &= \frac{1}{N} \sum_{i=1}^{i=N} x_i \\ \bar{y} &= \frac{1}{N} \sum_{i=1}^{i=N} y_i\end{aligned}\tag{2.17}$$

where N is the number of points on the spline.

$$A = \sum_{i=1}^{i=N} w \left(\sqrt{(x_{base,i} - x_i)^2 + (y_{base,i} - y_i)^2} \right)\tag{2.18}$$

where N is the number of points on the spline, $x_{base,i}$ and $y_{base,i}$ are the x and y coordinates of the base spline, x_i and y_i are the x and y coordinates of the spline being measured, and w is the width of the interval of t .

To get the best results for the area between the two curves, a sampling resolution had to be determined. A “good” sampling resolution will cause the width to be small enough to minimize the error in the area calculation. Figure 2.3 shows a graph of the area between two splines taken from the data used in the experiment. The area was found for different sampling resolutions from 30 points per spline to 30,000 points per spline. By looking at the data it was determined that 15,000 points would be more than sufficient as a sampling rate for our experiment. Results for this experiment can be seen in Section 3.2

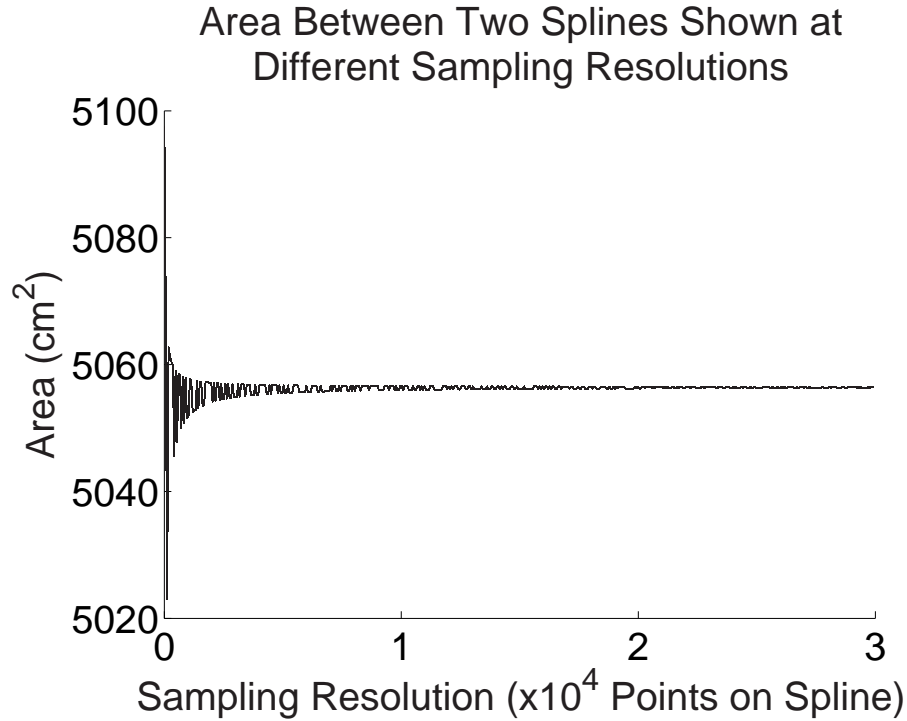


Figure 2.3: A plot showing the area between two splines at various sampling resolutions.

2.4 Data

Currently the data that is recorded from the shoothouse of the building clearing exercises is being cleaned manually. This means that someone goes through the entire file frame-by-frame and manually places the position of each member of the fireteam. Because the position data is accurate in these files, these files were used for the tests mentioned in Sections 2.2 and 2.3.

Figure 2.4 shows a 2-dimensional view of the shoothouse. All references to the fireteam motion and location will be done using this figure as a frame of reference.

For this experiment, three pieces of 10 separate clean files were used to test the spline extension methods and the team configuration method. When the building clearing exercise begins, the fireteam stacks in the far bottom right hallway against the left wall. Then they proceed around the corner and enter the first room on their left or the far right bottom room

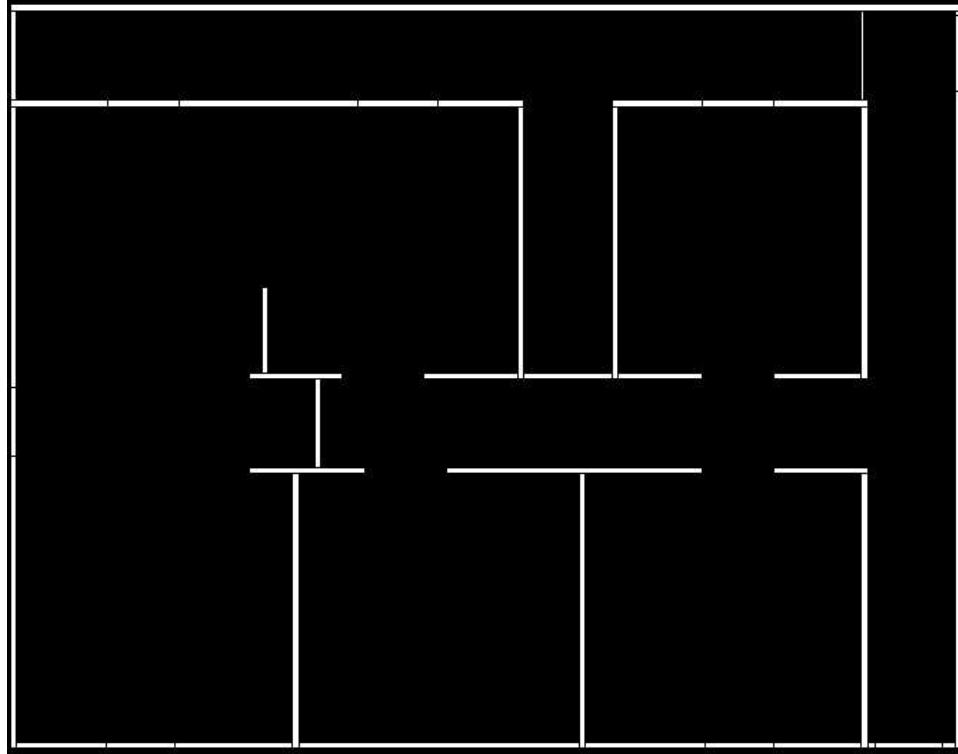


Figure 2.4: A 2-dimensional view of the shoothouse.

in Figure 2.4. The team then exits the room and proceeds through the rest of the house ³. This section of the clean file is then broken into 3 parts. The first part begins when the team stacks against the wall and continues until they arrive at the door of the first room. The second part consists of the entrance into the room. The final part consists of the entrance into the room but continues until the team exits the room.

³The entire path is not explained because their path up to exiting the first room is the only part relevant to the study.

Chapter 3

Results

3.1 Spline Extension Prediction Results

The results for the first experiment are presented in this section. Figures 3.1 through 3.6 show the results for the extension prediction for one of the trials. This is more for informational purposes to show a single trial, the average over all ten trial will be shown later and discussed more thoroughly. The results for trial 1 hall data can be seen in Figures 3.1 and 3.2, the entering the room data in Figures 3.3 and 3.4, and the full room data in Figures 3.5 and 3.6.

Figures 3.1 and 3.2 show the results for the hall data for trial 1. Figure 3.1 shows the average distance of the team positions away from the predicted positions using various curves in relation to time in the future, while Figure 3.2 shows the average distance of the team positions from the predicted positions using various curves in relation to average distance traveled by the team. In both graphs, the y-axis shows the average distance that the team positions differ from the predictions of the various curves. In Figure 3.1, the x-axis shows the time in the frames in the future, in which there are 20 frames per second. The x-axis of Figure 3.2 shows the average distance traveled by the team in centimeters.

Each of the graphs contains five different curves. The yellow line shows results for the straight line control curve. The black line shows the curve created by forming a spline with the four known control points and extending the final control point tangent with a straight line. The blue line shows the curve created by continuing the last section of the known spline with the same curvature. The red line shows the results of continuing the spline but dissipating the curvature of the last section of the known spline, while the green line shows results of increasing the curvature of the last section.

This breakdown of the two graphs for each figure is exactly the same for the entering the room data in Figures 3.3 and 3.4 and the complete room data in Figures 3.5 and 3.6. These six figures show the results for all three data sets for a single trial.

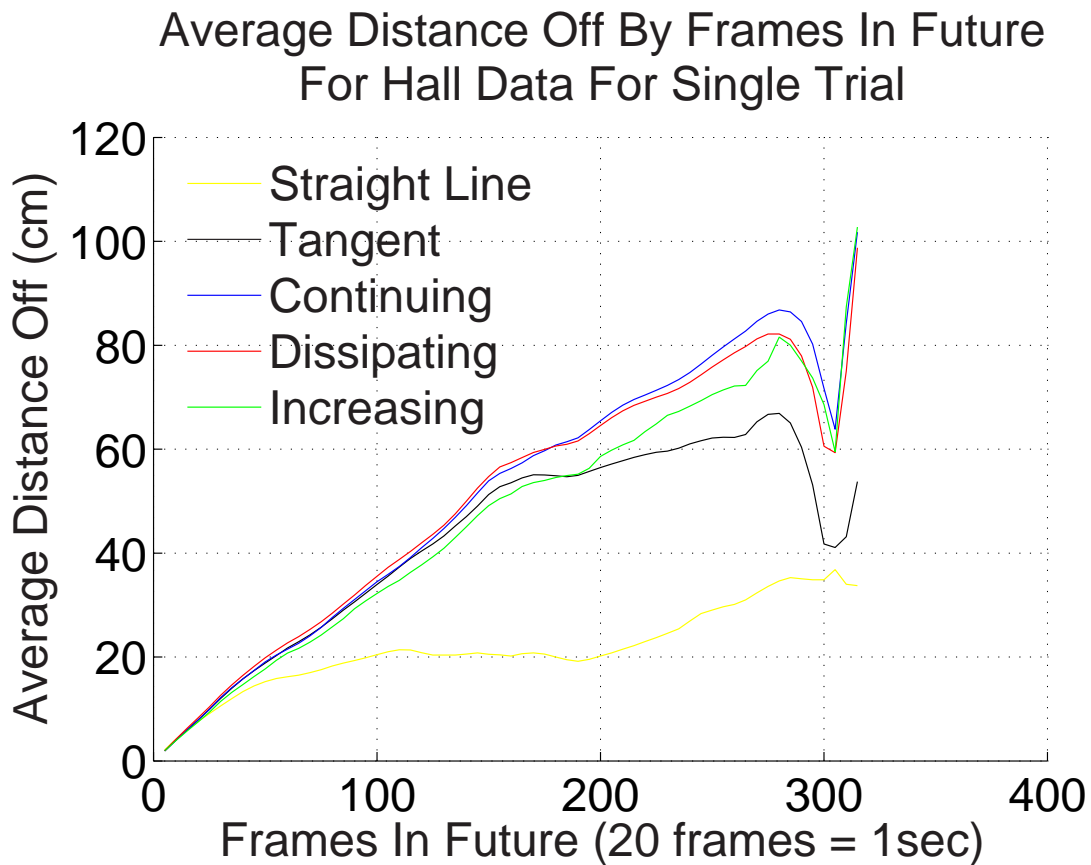


Figure 3.1: Frame extension results for trial 1 hall data.

Although the single trial results are more for informational purposes, it is necessary to discuss the noise that occurs in the plots of the average distance off by average team

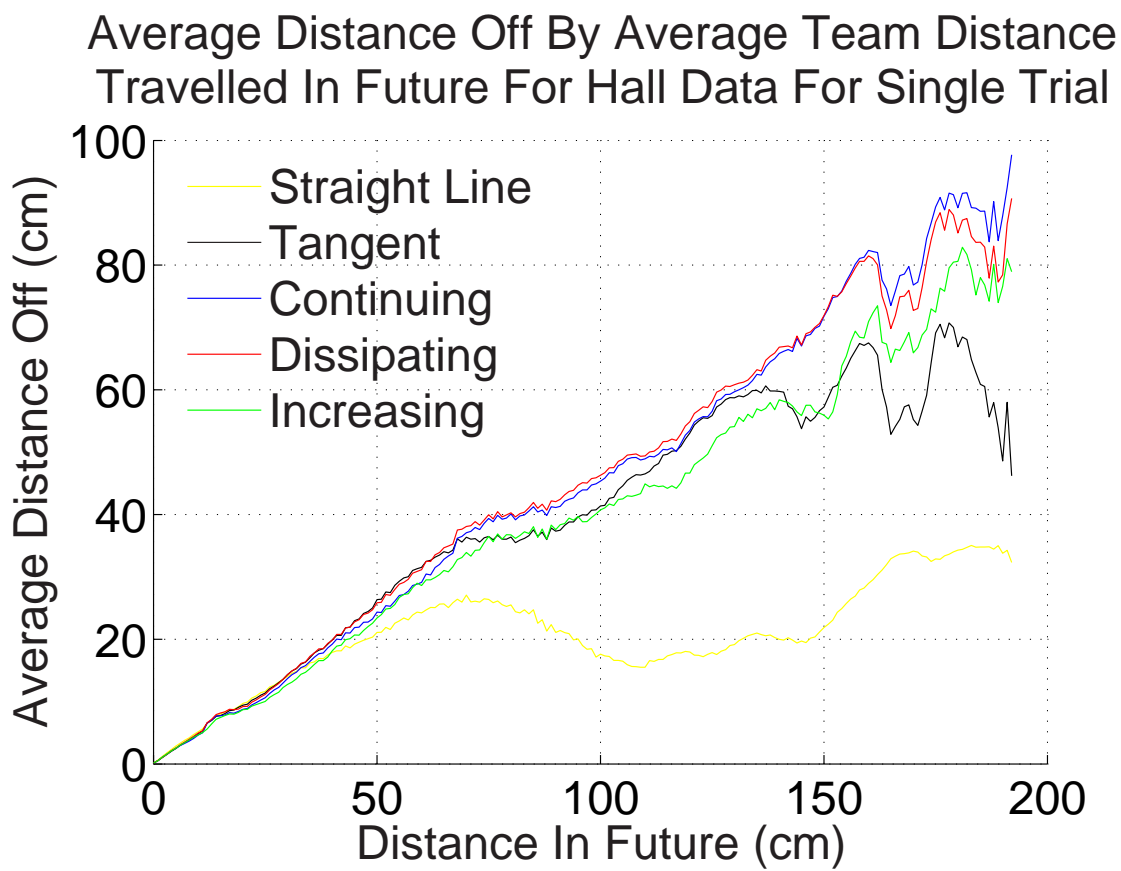


Figure 3.2: Distance traveled extension results for trial 1 hall data.

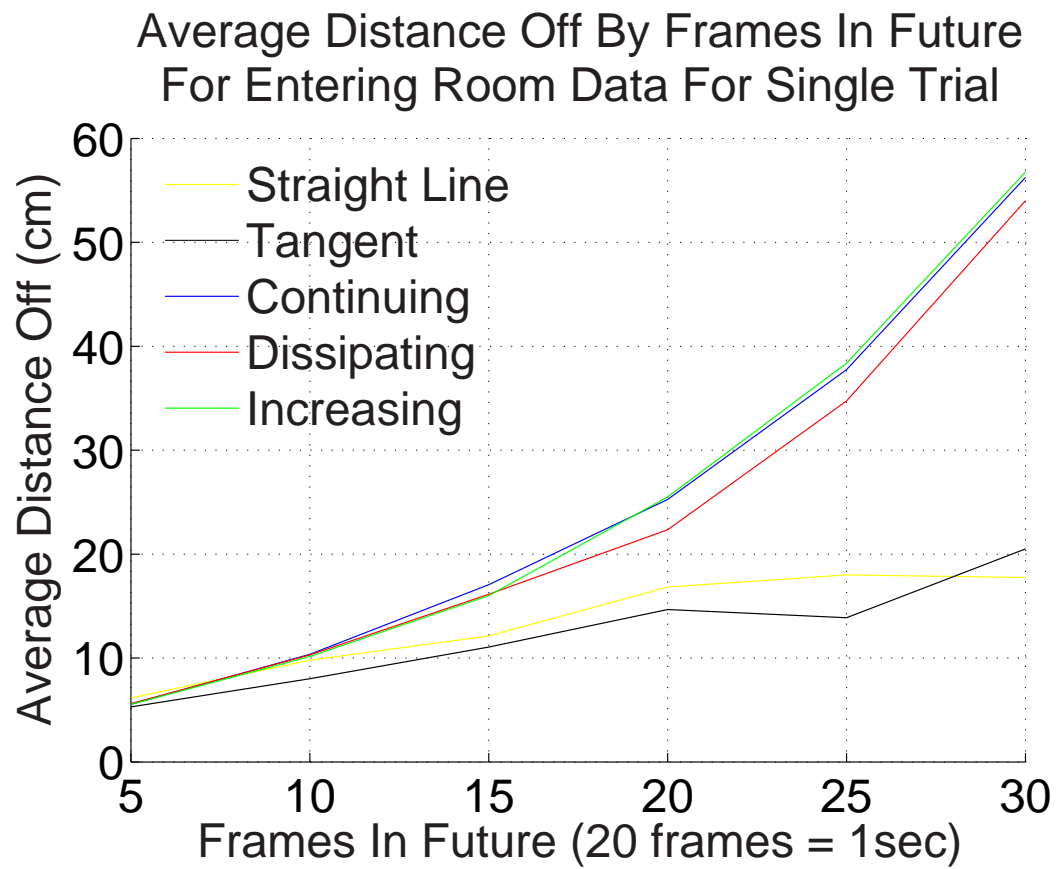


Figure 3.3: Frame extension results for trial 1 entering room data.

Average Distance Off By Average Team Distance Travell In Future For Entering Room Data For Single Trial

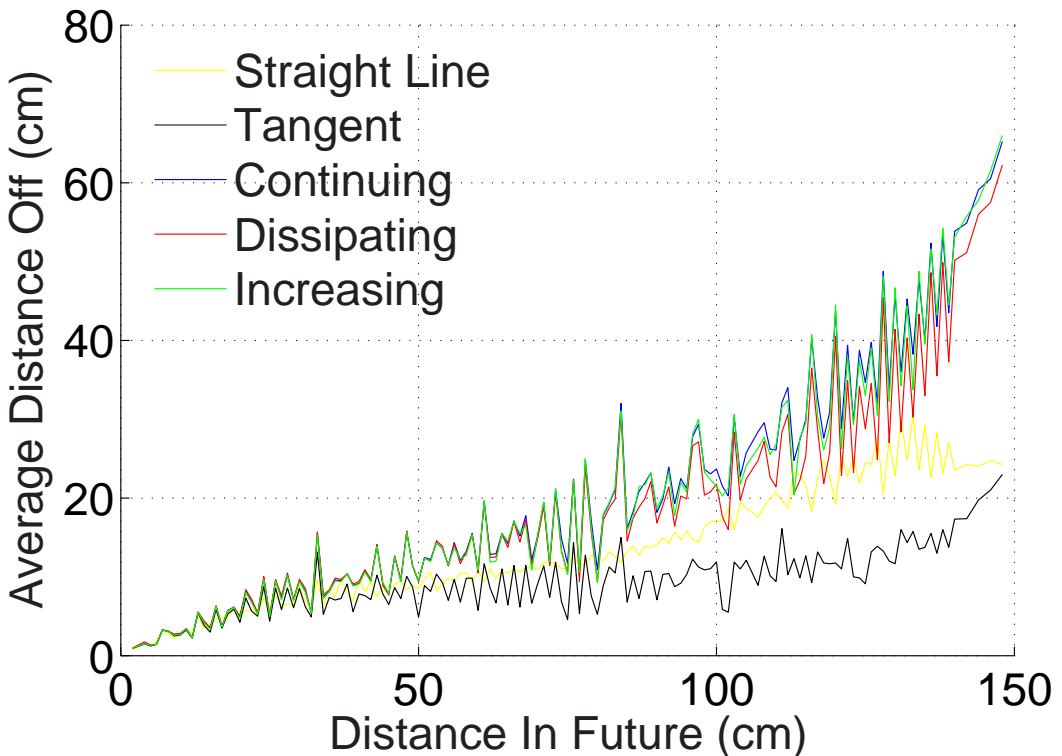


Figure 3.4: Distance traveled extension results for trial 1 entering room data.

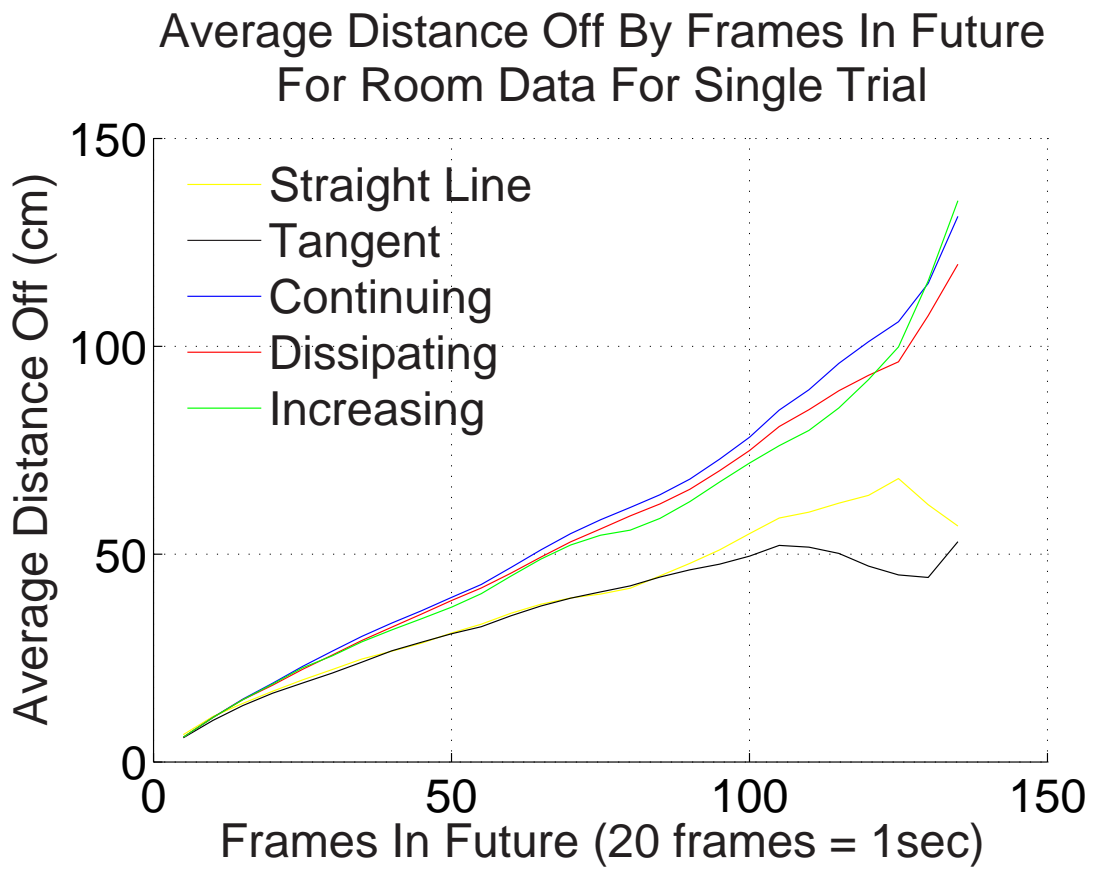


Figure 3.5: Frame extension results for trial 1 room data.

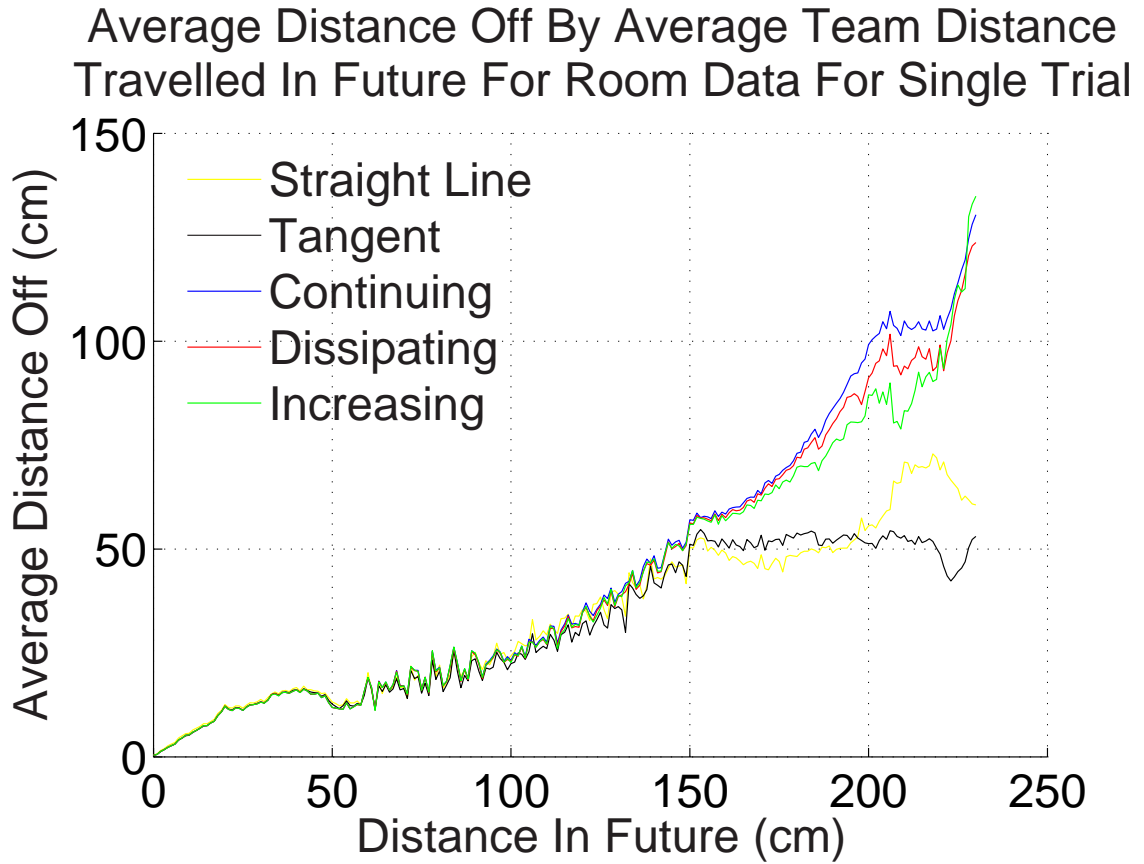


Figure 3.6: Distance traveled extension results for trial 1 room data.

distance traveled plots. This noise is much more prevalent in some plots than others, especially the entering the room data. Although only one trial is shown here, this noise occurs throughout all of the trials. This noise is due to the varying number of points (or lack thereof) for each average distance measurement traveled by the team. This variation in the number of points causes the noise and prevents the smoothing of the curve that is seen in the plots for the distance off for time in the future. Figure 3.7 shows a plot of the number of data points for each centimeter of average distance traveled by the team for the dissipating curve of the room entering data shown in Figure 3.4.

Appendix A shows the graphs of the average distance off for all three data sets averaged over all ten trials for time and distance in the future. Because we want to track within 5-10 cm of accuracy it can be seen in these plots that most of the data is useless to our research. However, for short team distances traveled or a few frames into the future, the data is

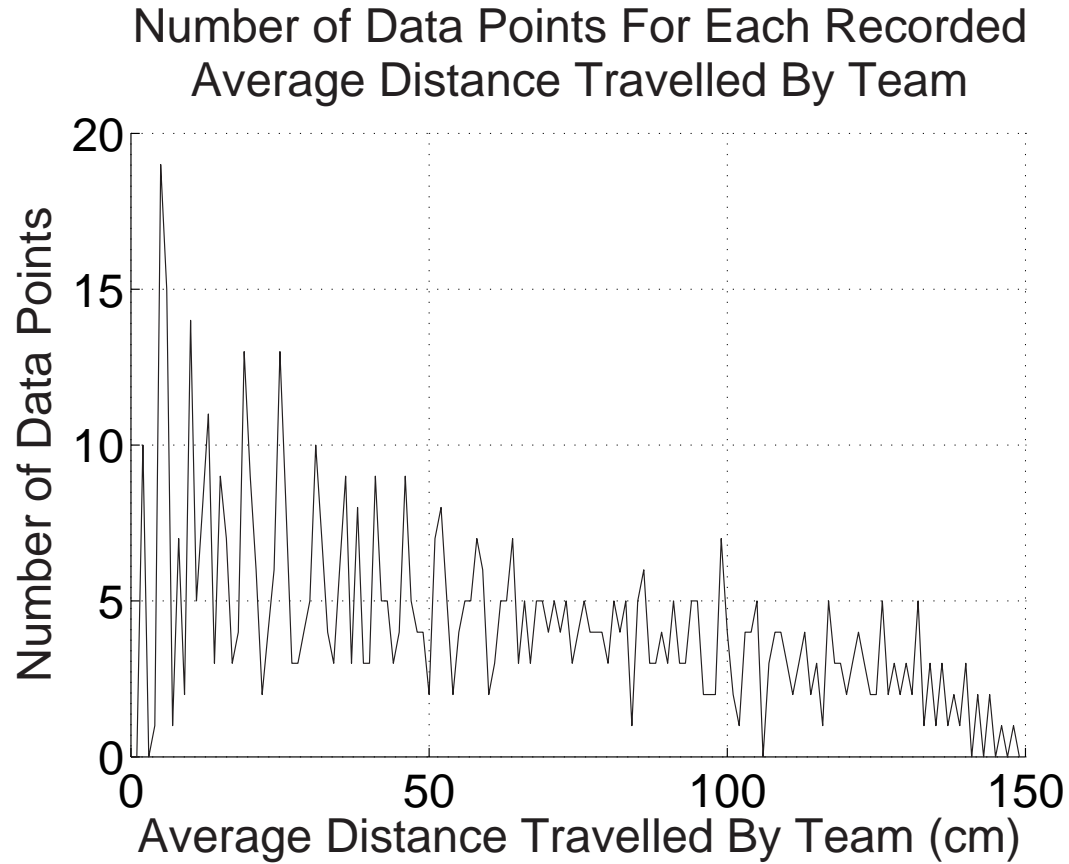


Figure 3.7: Total data points for each distance in the trial 1 room entering data file.

helpful. A zoomed in view of these plots in which the data is useful to our research will be discussed later.

Although the results in the plots in Appendix A, for the most part, do not pertain to our needs in particular, there are some interesting observations that can be made from these plots. These plots are similar to those of the single trial. They are broken down into the three data sets in which the average distance is measured on the y-axis, and either time or average distance traveled by the team is on the x-axis. Each plot shows all five curves that were extended to predict future motion.

The first observation made is that by looking at these plots, in the area that is useful to our particular research seems to show that all curves are almost exactly the same. This will be discussed later with the zoomed in plots. The second observation is how the particular curves perform farther into the future than is beneficial to our research. This is the area

where the curves begin to separate. In the hall data, for both time and distance in the future, the straight line control curve seems to be the best choice. This result makes sense since in the hall the fireteam is lined up against the wall and follows the wall in a straight line. However, for the entering the room data and the entire room data, the straight line control curve is the worst. For these two data sets, increasing the curvature as the curve is extended did better for the entering the room because the first member of the fireteam was taught to button-hook into the room. Also, for the entire room data, the increasing curvature extension shows slightly better results due to the way the team is taught to enter and cover the entire room. Although these results are not useful to our research due to the small amount of error allowed, they could be useful in larger projects in which the allowed accuracy error is greater.

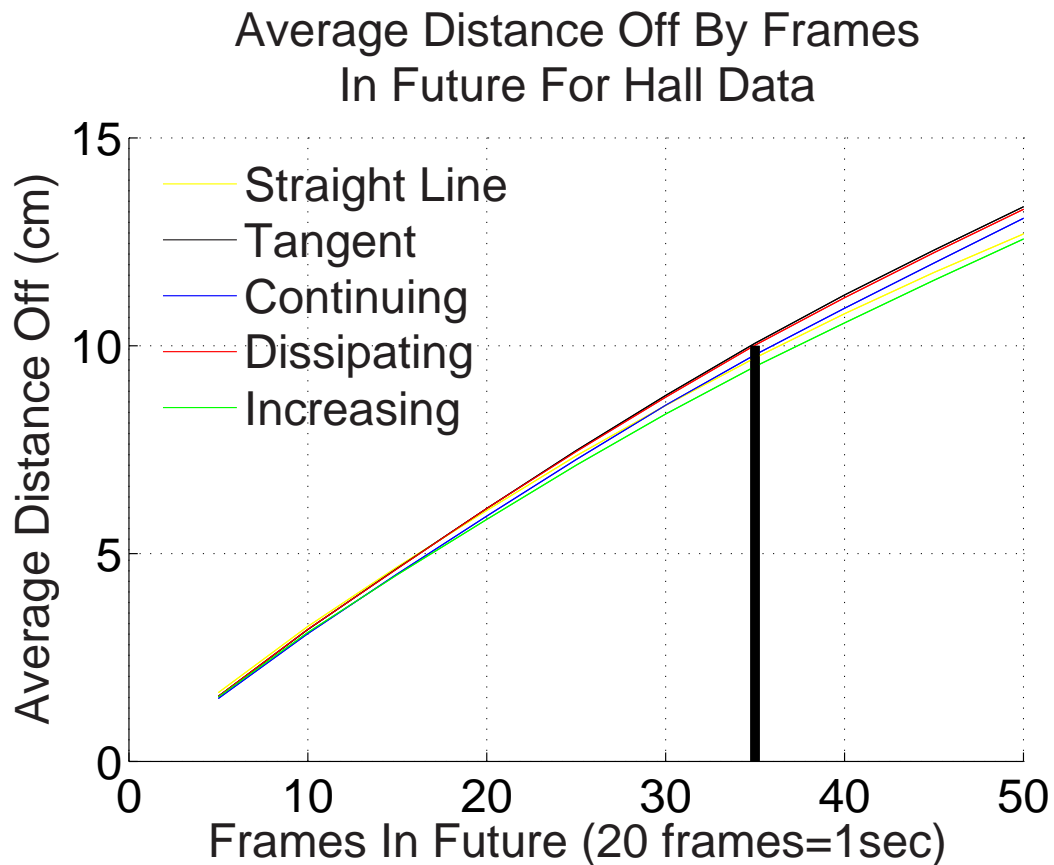


Figure 3.8: Average distance from curve for time in future for hall data.

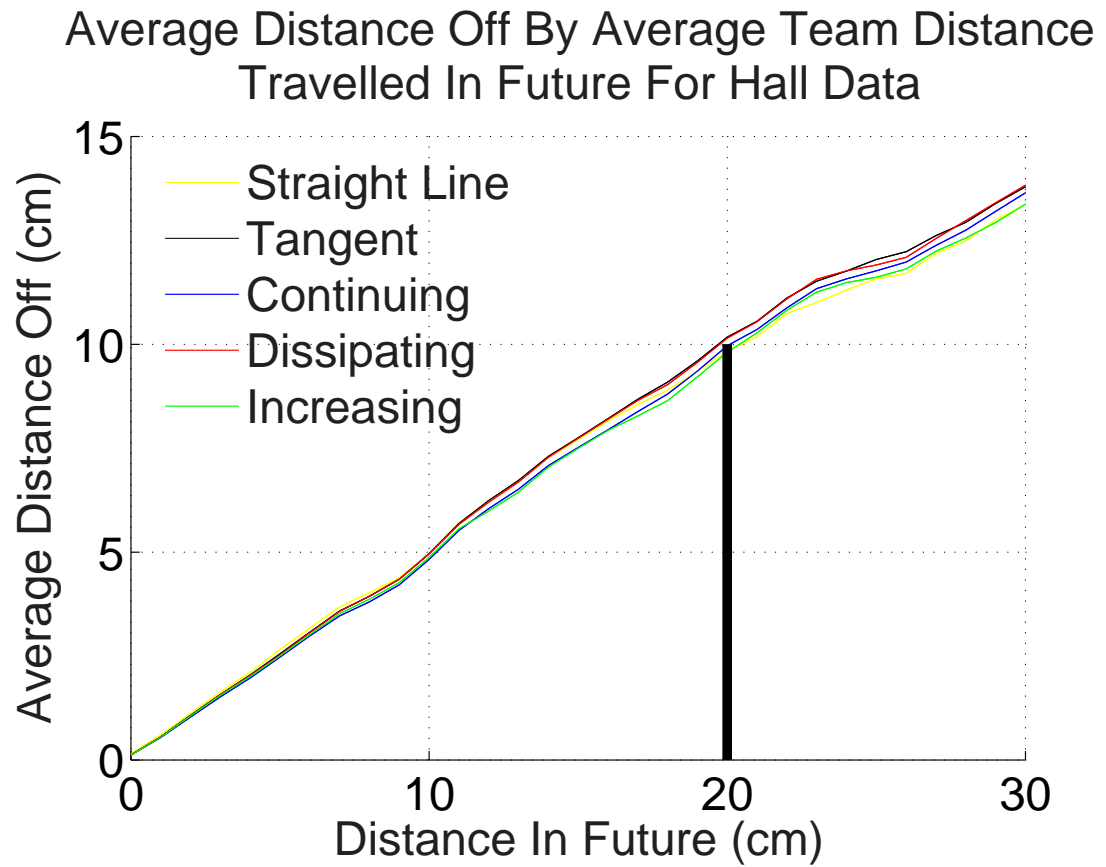


Figure 3.9: Average distance from curve for team distance traveled in future for hall data.

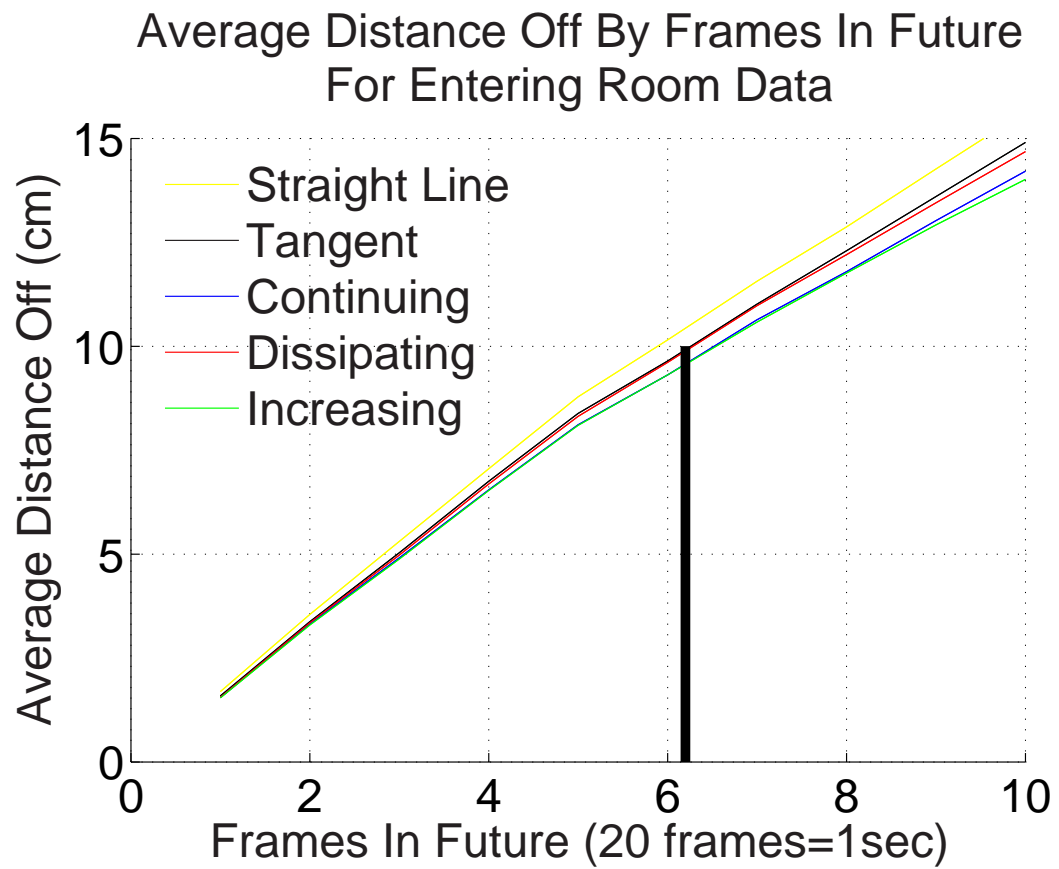


Figure 3.10: Average distance from curve for time in future for entering data.

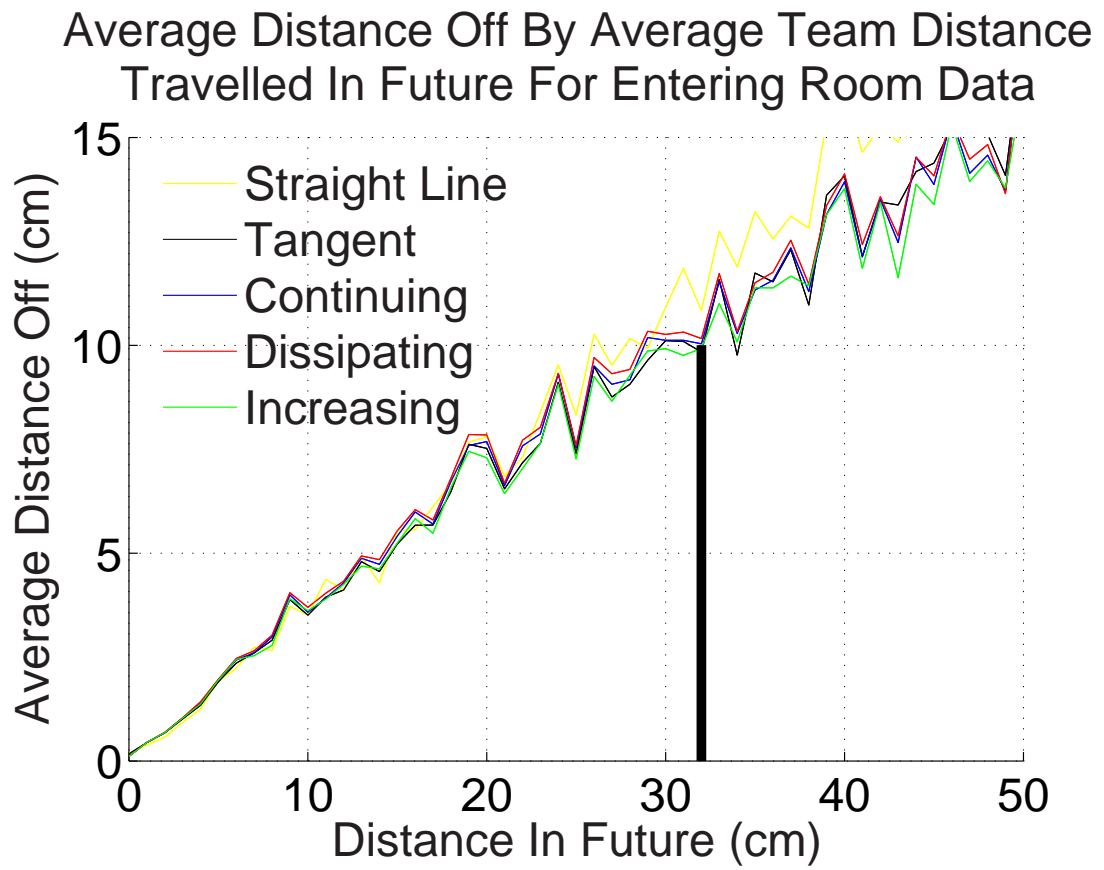


Figure 3.11: Average distance from curve for team distance traveled in future for entering data.

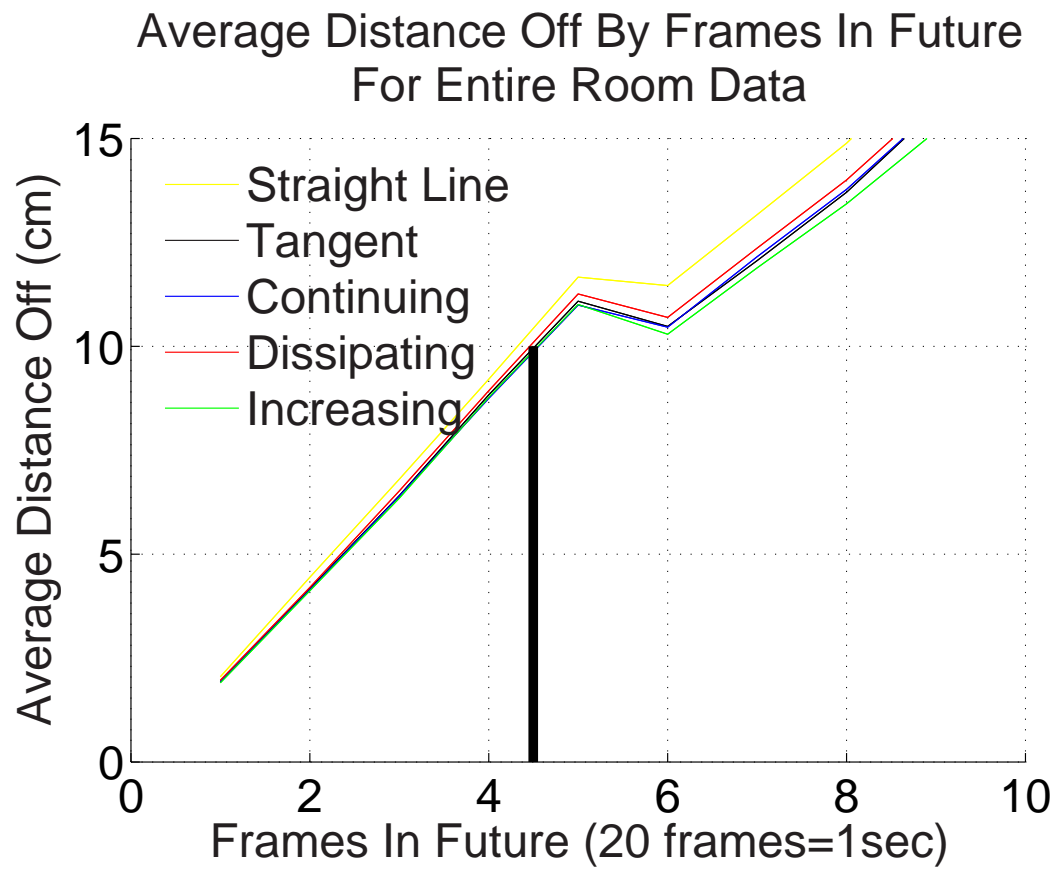


Figure 3.12: Average distance from curve for time in future for room data.

Average Distance Off By Average Team Distance Travelled In Future For Entire Room Data

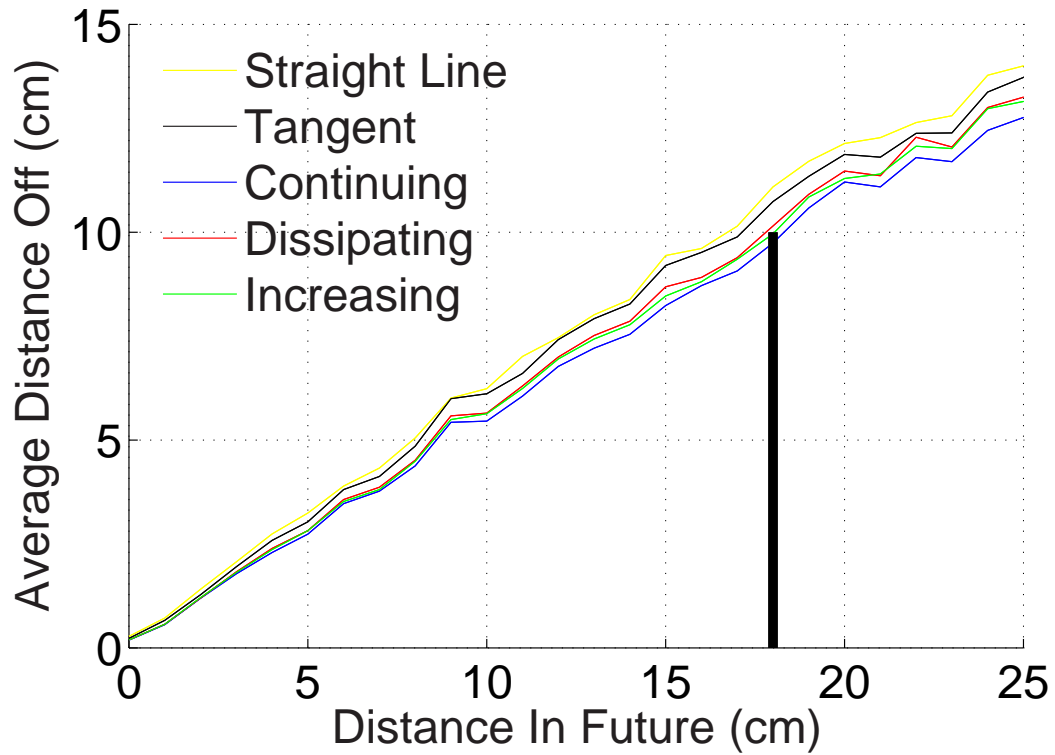


Figure 3.13: Average distance from curve for team distance traveled in future for room data.

Figures 3.8 through 3.13 show the zoomed in results for the average distance off of the predicted positions for time and average distance traveled by the team in the future. These plots show the 10 cm accuracy error that is allowed for our research. Figures 3.8, 3.10, and 3.12 show the distance off in reference to frames in the future, where 20 frames = 1 second, and Figures 3.9, 3.11, and 3.13 show the distance off in average distance traveled by the team in centimeters. The x-axes are labeled accordingly. The y-axes for the plots show the average distance off from the predicted positions of the ten trials in centimeters. Each plot shows all five of the extension curves, where the yellow line represents the straight line control curve, the black line shows the straight line tangent extension, the blue line shows the continuous curvature extension, the red line show the dissipating curvature extension, and the green line shows the increasing curvature extension.

	Frames (20 Hz)	Seconds	Distance (cm)
Hall Data	35	1.75	20
Entering Room Data	6.2	0.3	32
Entire Room Data	4.5	0.2	18

Table 3.1: Results of the position prediction experiment.

In the zoomed in figures, the separation of the curves is a little easier to see than in the full graphs in appendix A. In both of the hall data plots, it can be seen that even though there is some separation, it is minimal. This is due to the fact that the team is lined up against a wall and the curves are close to straight lines. Therefore, the predicted paths are very similar and give similar results. For both the entering the room data and the entire room data, the curves are also close together. This is caused by the small amount of time and short average distances traveled in the future. The extensions are relatively close for such small numbers. However it is noticeable that for both of these data sets in which future motion of the team involves curving, the straight line control curve is the worst for predicting future motion.

The results from the six zoomed in plots of the average distance off of the predicted positions can be seen in Table 3.1. This table shows the amount of time or average distance traveled by the team in to the future the extension curves can predict before exceeding the allowable error. For the hall data, the positions can be predicted for 35 frames or almost 2 seconds into the future, however, the distance is only 20 cm. This large time, small distance is due to the fact the the team spends a lot of time in the same location preparing to move. The entering the room results show that the positions can be predicted for 32 centimeters but for only approximately 6 frames, or approximately 0.3 seconds. This is due to the fact the this data consists of a quick burst into the room in which the team has a much higher velocity than in the hall and “follow the leader” on a curve relatively closely. The entire room data has the lowest results for both time and distance traveled at between 4 and 5

frames, or 0.2 to 0.25 seconds, and 18 cm because when the team enters the room they quickly split up to cover the entire room.

3.2 Configuration Retention Results

This section discusses the spline shape retention, or how well the team retains its configuration, results. Figure 3.14 shows the results of how well the team retained the same configuration over time. The y-axis shows the average area of the ten trials between the two spline curves. The x-axis shows the time in the future between the two curves in frames, where 20 frames represent one second. In this graph, there are three plots. The yellow plot shows the results for the hall data, the blue plot shows the results for the entire room data, and the black plot shows the results for the data of the team entering the room. Figure 3.15 shows the results for the area between the curves based on average distance traveled by the team. The breakdown of the graph is the same except the x-axis represents the average distance traveled by the team in centimeters.

Figures 3.14 and 3.15 are almost exactly alike. This is caused for two reasons in the hall data. First they are moving slowly, so that there is little change in distance in five frames (0.25 seconds). This means that most of the average distances traveled by the team are covered in the five frame, or 0.25 second, advances in time. Also the team is moving with relatively constant velocity without changing configuration very much, so that even though the initial configurations used in the comparisons may fall at different times, the area between configurations are similar. For the room entering data, the amount of time and distance covered is minimal and few measurements are taken, so the graphs appear similar. The room data is similar to the hallway data with relatively constant velocity and relatively slow movement. This causes the average over the ten trials to produce similar areas between configurations graphs.

Average Area Between Current Configuration and Future Configuration By Time

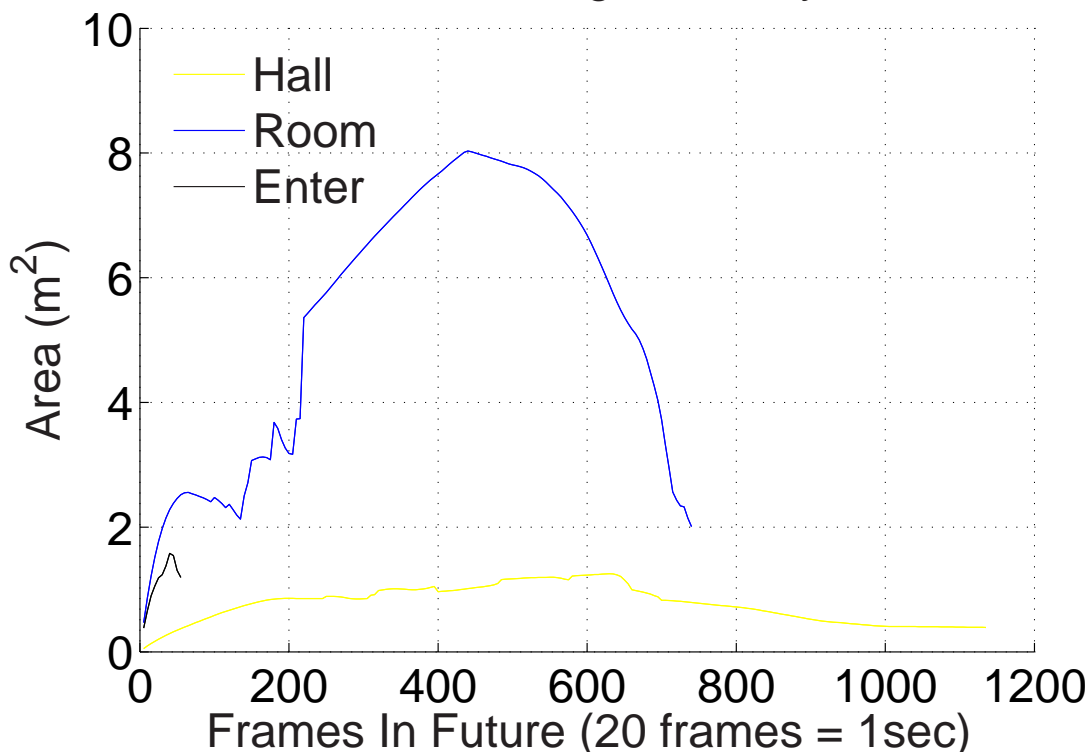


Figure 3.14: Average area between configurations based on time.

The results for the three data set are what was expected. The hall data is the lowest and remains at approximately 1 m². This is due to the fact that the team remains in a relatively straight line and follows the leader to the door of the first room as they ready themselves to enter. The “bump” that can be seen at approximately 100 frames (5 seconds) or 500 cm is caused by the team rounding the corner in the hallway. They stay close to a line and about the same distance apart, however, their formation changes from a straight line to a curved shape around the corner. The decline at the end of the data set is due to the fact that the beginning of the data in which the team is spread out is being compared to the end in which the team is bunched together preparing for movement. Although the configuration has rotated 90 degrees, the team is bunched together to bring the calculated area down. The entering the room data increase quickly because this is the burst into the room. The team starts to spread out and move from a straight line configuration to a curve around the door.

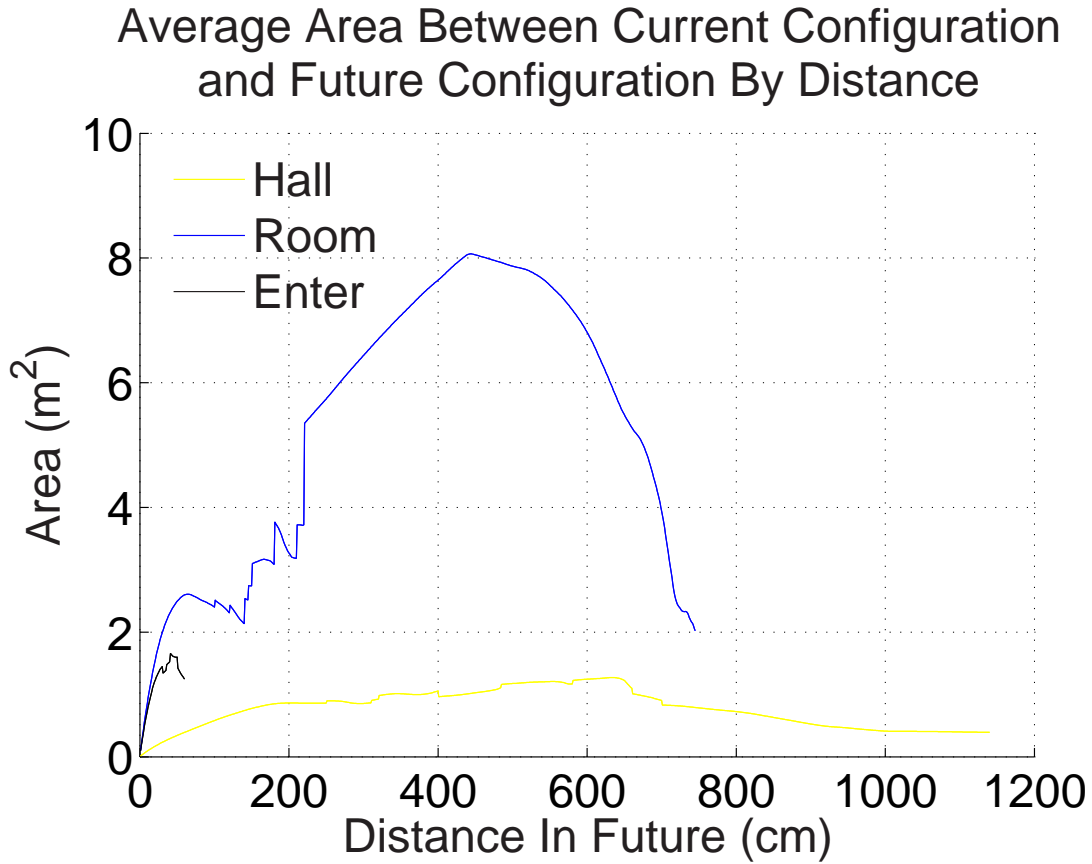


Figure 3.15: Average area between configurations based on average distance traveled.

The decline at the end of the plot is due to the fact that as the team rounds the corner, the team members begin to move closer to each other, even though the wall is between them so the area decreases. The room results are the largest as expected because the team spreads out to the corners of the room to cover the entire area of the room. The decline at the end of the graph is caused by the team beginning to exit the room and move back towards a straight line configuration which brings the area difference down.

Although the results are what was expected, it is hard to visualize the area between the two formations and what kind of team movement is involved. Figure 3.16 shows the team movement that causes a 0.17 m^2 change in area, Figure 3.17 shows the movement of the team in which the configuration change is approximately one square meter and Figure 3.18 shows the position change in which the configuration change is approximately five square meters. In the three figures the x-axes represent the floor-plane x- axis at the shoothouse

and the y-axes represent the y-axis. The blue curve shows the current spline representation of the team configuration while the black curve shows a future configuration. Figures 3.16 and 3.17 show the team as they move down the hallway to a future location in which the change in configuration is approximately 0.17 m^2 and 1 m^2 , respectively. Figure 3.18 shows the team initially spread out throughout. As the team moves towards the door to exit the room the configuration changes enough to cause a 5 m^2 difference.

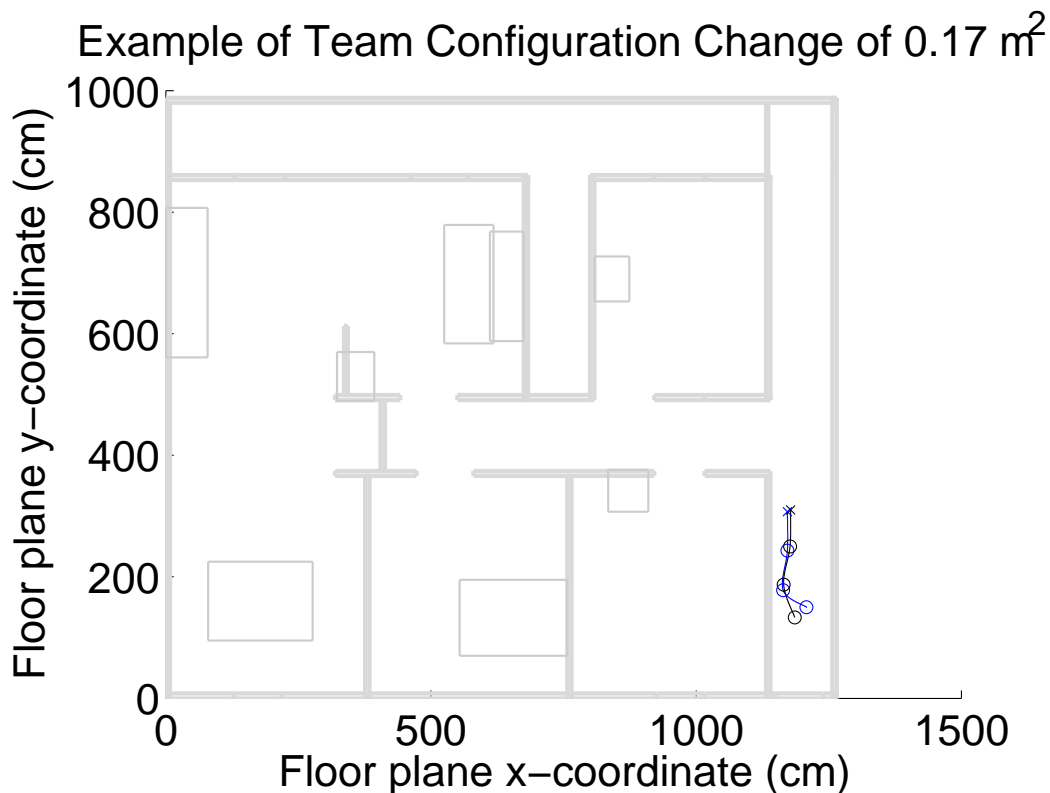


Figure 3.16: Example of a 0.17 m^2 change in configuration.

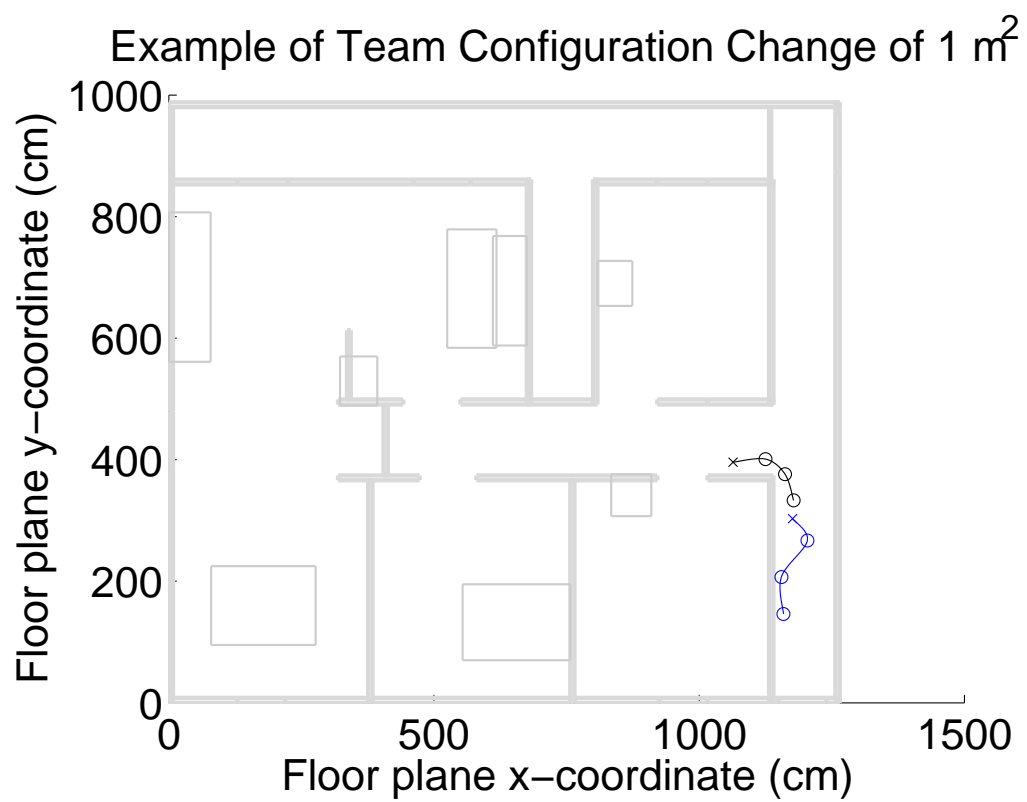


Figure 3.17: Example of a 1 m² change in configuration.

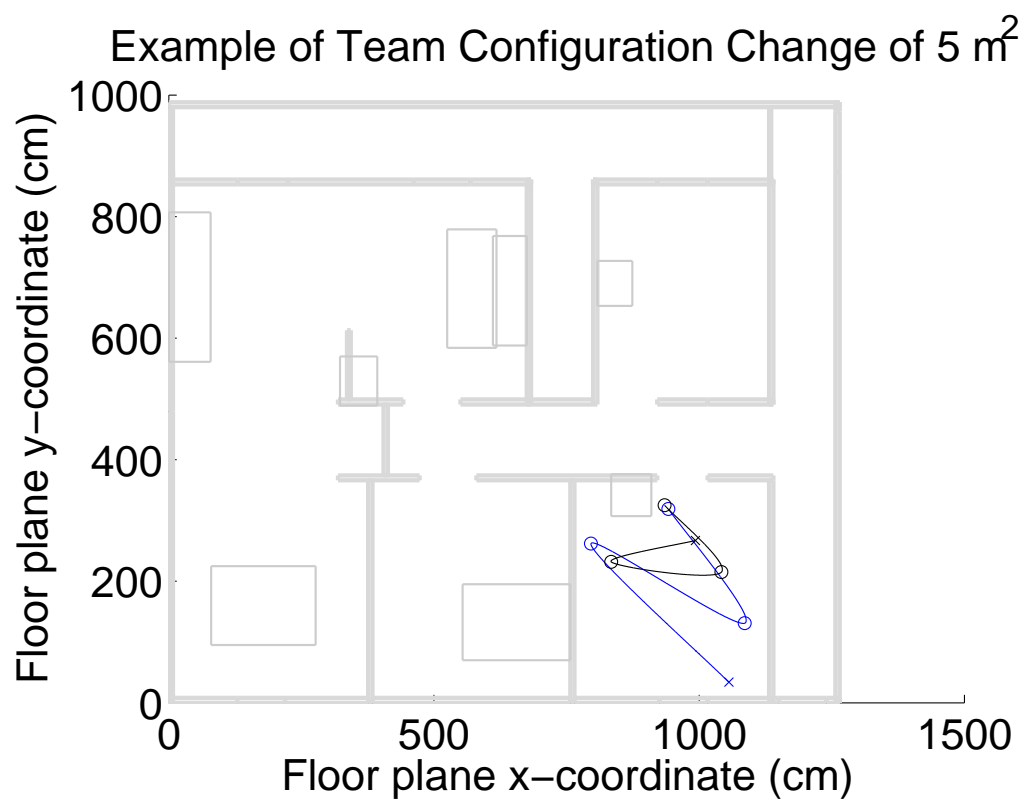


Figure 3.18: Example of a 5 m² change in configuration.

Chapter 4

Conclusions

This paper presented a way to track the positions of a fireteam (4 -5 men) as they perform building clearing exercises in order to predict future motion of the team. This was done by examining the team as a single entity rather than 4 or 5 separate entities. A team model was used under the assumption that the team stays together as a group and moves in specific patterns. The model chosen for this experiment was a spline curve. This spline curve allowed for movement in straight lines through hallways as well as curving around corners.

Two experiments were conducted to help predict the future motion of the team. The first experiment extended the curve created by the current team member positions. Five different extensions were examined: a straight line extension, a straight line extension from the tangent formed at the last team member, a curve in which the curvature of the spline remained the same through the extension, a curve in which the curvature dissipates through the extension, and a curve in which the curvature increases through the extension. The distance of the team from the predicted line was measured. The second experiment performed measured how well the team retained their configuration as they moved. This was done by taking the area difference between the spline created at the current location and the spline at future locations.

The results of the experiment show that applying a geometric model to the team and examining their movement as a whole instead of separate entities can be useful in predicting the future positions of the team members. In a hallway, extending the curve does well for predicting time into the future, but not as well for distance. This happens since the team moves slow and instead of following each other, they move out of line to peek around corners and each other. However, even though they do move out of line to peek, their configuration remains relatively the same. As for entering the room, the extension methods do well for distance. This means that team does a good job of playing “follow-the-leader” into the room. The configuration changes due to the quick acceleration of the team, however it is mainly caused by a “stretching” of the team configuration. For the room data the prediction method for movement is minimal due to the fact that they spread out to cover the entire room. This also causes a large change in configuration.

Overall, the spline model shows merit in predicting the team’s future positions as they enter the room. While in the room, it is hard to predict the future motion since the team spreads out so much to cover all the corners. Although, in some places, the spline extension method was able to predict future positions, the different types of extensions performed relatively equally. Even though some were better and some were worse, the differences did not cause enough change in the results for our limited error to choose one extension as the best. As for the configuration, even though the team moves from formation to peek around corners and see around each other they remain close to the same configuration and move slowly. This can be useful in predicting their motion over time.

To our knowledge, this work is the first to apply a team model to tracking during building clearing exercises. Using a spline to model the team allowed for predictions of future positions and configurations. The experiments show that the idea of applying a geometric model to the team has merit, but warrants further development. In particular, other geometric models could be tried to improve the predictions for other areas of the building. Also, correction factors from raw data collected, which were not used, could be applied to

the calculations to increase prediction distances and times. The orientation of the team as they move through the building based on location or the orientation measurements taken from other devices could be used in configuration predictions. Integrating the configuration changes and predictions with the extension methods could also allow for better position predictions. This is just the first step to improve future position predicting using a team model.

Bibliography

- [1] A. Ahuja. Determining battlefield effects in an urban environment: Mout terrain analysis. *Military Intelligence Professional Bulletin*, 29(3):28–31, July-Sept 2003.
- [2] L. Akins and D. Barbuto. Work in progress: Preliminary analysis of developing team building skills in community college students. *Proceedings - Frontiers in Education Conference*, 3:S3G–24–S3G–25, 2004.
- [3] A. Blake and M. Isard. *Active Contours*. Springer, 1998.
- [4] M. Blake, G. Sorenson, J. Archibald, and R. Beard. Human assisted capture-the-flag in an urban environment. *Proceedings - IEEE International Conference on Robotics and Automation*, 2004(2):1167–1172, 2004.
- [5] F. Borsato and F. Flores. A real-time method to object detection and tracking applied to robot-soccer. *2004 IEEE Conference on Cybernetics and Intelligent Systems*, pages 174–178, 2004.
- [6] J. Brooks. Trip report as the us service and us army representative to the nato fibua (fighting in built up areas) working group. *Stockholm, Sweden*, 13-16 April 2004.
- [7] J. Bruce. Design methodology suitable for team-based embedded systems education. *Computers in Education Journal*, 14(3):41–54, July/September, 2004.
- [8] D. Burgess. High-speed particle tracking probes turbulent flows. *Photonics Spectra*, 40(4):74–75, April, 2006.
- [9] T. Chen and R. Luo. Multilevel multiagent based team decision fusion for mobile robot behavior control. *Proceedings of the World Congress on Intelligent Control and Automation*, 1:489–494, 2000.
- [10] D. Cummins. Using competition to build a stronger team. *Proceedings of the Agile Development Conference*, pages 137–141, 2004.
- [11] S. Damiani, G. Verfaillie, and M.-C. Charneau. An earth watching satellite constellation: How to manage a team of watching agents with limited communications. *Proceedings of the 4th International Conference on Autonomous Agents and Multi Agent Systems*, pages 589–596, 2005.

- [12] M. Di Marco, A. Garulli, A. Giannitrapani, and A. Vicino. Simultaneous localization and map building for a team of cooperating robots: A set membership approach. *IEEE Transactions on Robotics and Automation*, 19(2):238–249, April, 2003.
- [13] R. Drew, A. Dubuisson, B. Milligan, J. Williams, S. Beyerlein, E. Odom, and K. Rink. Early development of capstone design teams through graduate student mentoring and team building activities. *2003 ASEE Annual Conference and Exposition: Staying in Tune with Engineering Education*, pages 9615–9625, 2003.
- [14] D. DuPont. Inner-city violence. *Scientific American*, pages 39–40, October 1998.
- [15] J. Foley, A. van Dam, S. Feiner, and J. Hughes. *Computer Graphics Principles and Practice*. Addison-Wesley Publishing Company, Inc., 1996.
- [16] K. Geis. Photonics and instrumentation for real-time monitoring of the u.s. army’s ft. polk, louisiana, joint readiness training center’s military operations in urban terrain complex. *Proceedings of SPIE - The International Society for Optical Engineering*, 2497:192–199, 1995.
- [17] D. Gibson, B. Ling, M. Zeifman, S. Dong, and U. Venkataraman. Multipedestrian tracking. *Public Roads*, 69(5), March/April, 2006.
- [18] A. Hoover and E. Muth. A real-time index of vagal activity. *International Journal of Human-Computer Interaction*, 17(2):197–209, 2004.
- [19] M. Jamzad and A. Lamjiri. Towards an intelligent vision system for mobile robots in robocup environment. *IEEE International Symposium on Intelligent Control - Proceedings*, pages 1012–1017, 2003.
- [20] O. Kannianen, S. Menani, J. Matila, and N. Ould-Khessal. Fast dynamic object tracking in a robotic soccer team. *Proceedings of the IASTED International Conference on Robotics and Applications*, pages 13–17, 2003.
- [21] E. Muth, A. Hoover, and M. Loughry. Developing an augmented cognition sensor for the operational environment: the wearable arousal meter. *proceedings of HCI International*, 2005.
- [22] J. Spletzer and C. Taylor. Dynamic sensor planning and control for optimally tracking targets. *International Journal of Robotics Research*, 22(1):7–20, January, 2003.
- [23] S. Teasley, L. Covi, M. Krishnan, and J. Olson. How does radical collocation help a team succeed? *Proceedings of the ACM Conference on Computer Supported Cooperative Work*, pages 339–346, 2000.
- [24] M. Veloso, P. Stone, and K. Han. Cmunitied-97 robotic soccer team: Perception and multiagent control. *Proceedings of the Interantional Conference on Autonomous Agents*, pages 78–85, 1998.

- [25] K. Waller, J. Luck, A. Hoover, and E. Muth. A trackable laser tag system. *WORLD-COMP'06 The 2006 International Conference on Computer Games*, June 26-29, 2006.
- [26] Z. Wang, E. Nakano, and T. Takahashi. Solving function distribution and behavior design problem for cooperative object handling by multiple mobile robots. *IEEE Transactions on Systems, Man, and Cybernetics Part A: Systems and Humans*, 33(5):537–549, September, 2003.
- [27] Wikipedia. Spline (mathematics). Available on: http://en.wikipedia.org/w/index.php?title=Spline_28mathematics%29&oldid=58419909, 2006. [Online; accessed 10-August-2006; Last modified June 13, 2006].

APPENDICES

Appendix A

Entire Extension Graphs

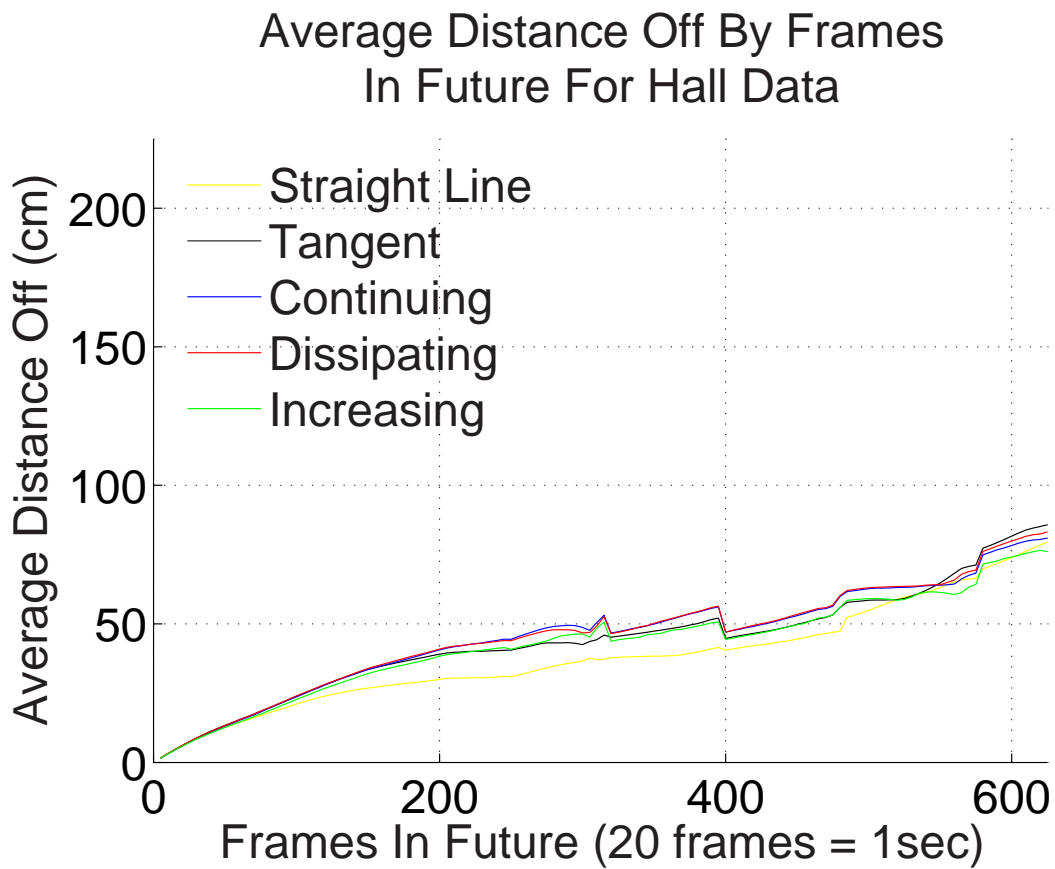


Figure A.1: Entire average distance from curve by frames graph for hall data.

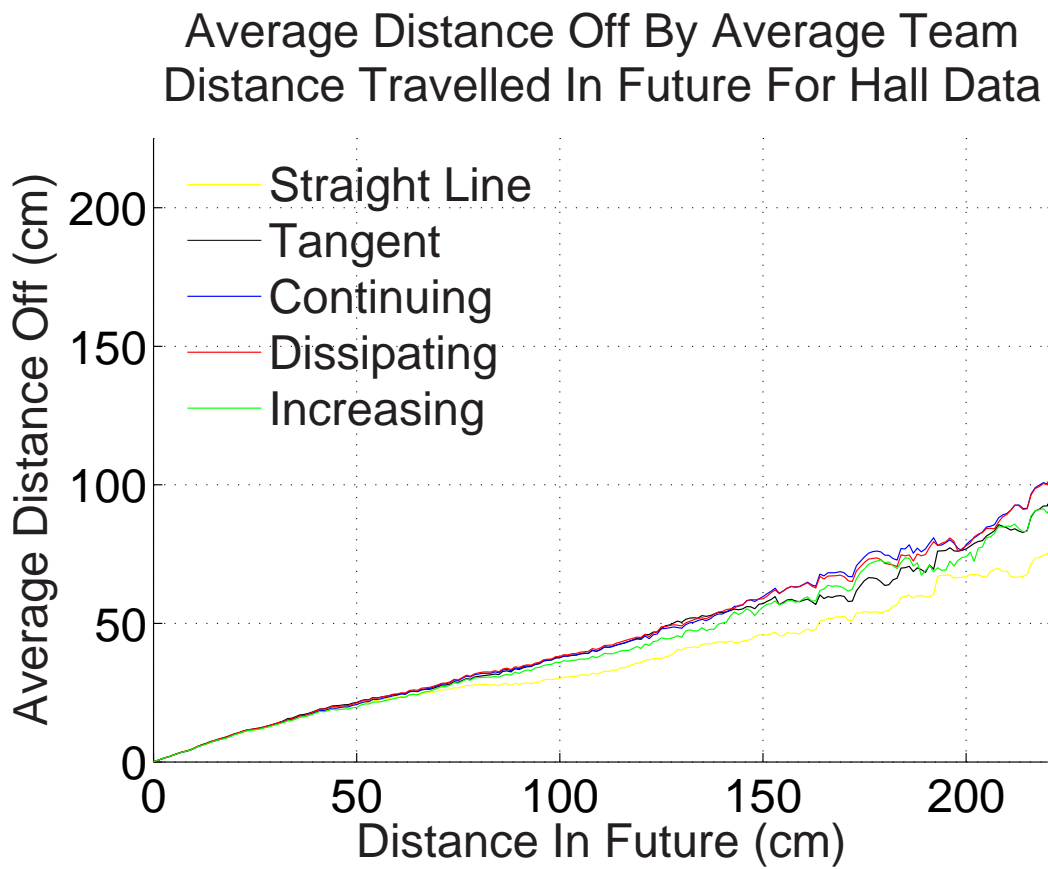


Figure A.2: Entire average distance from curve by distance graph for hall data.

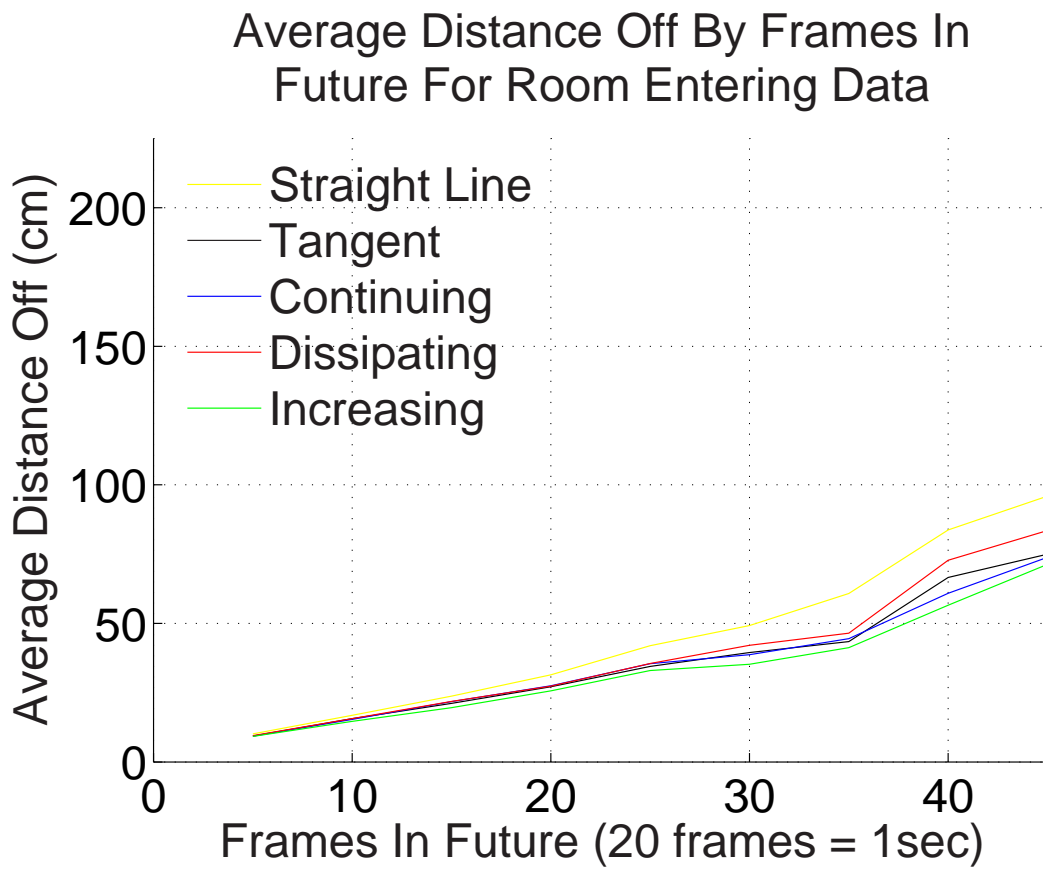


Figure A.3: Entire average distance from curve by frames graph for room entering data.

Average Distance Off By Average Team Distance Travelled In Future For Room Entering Data

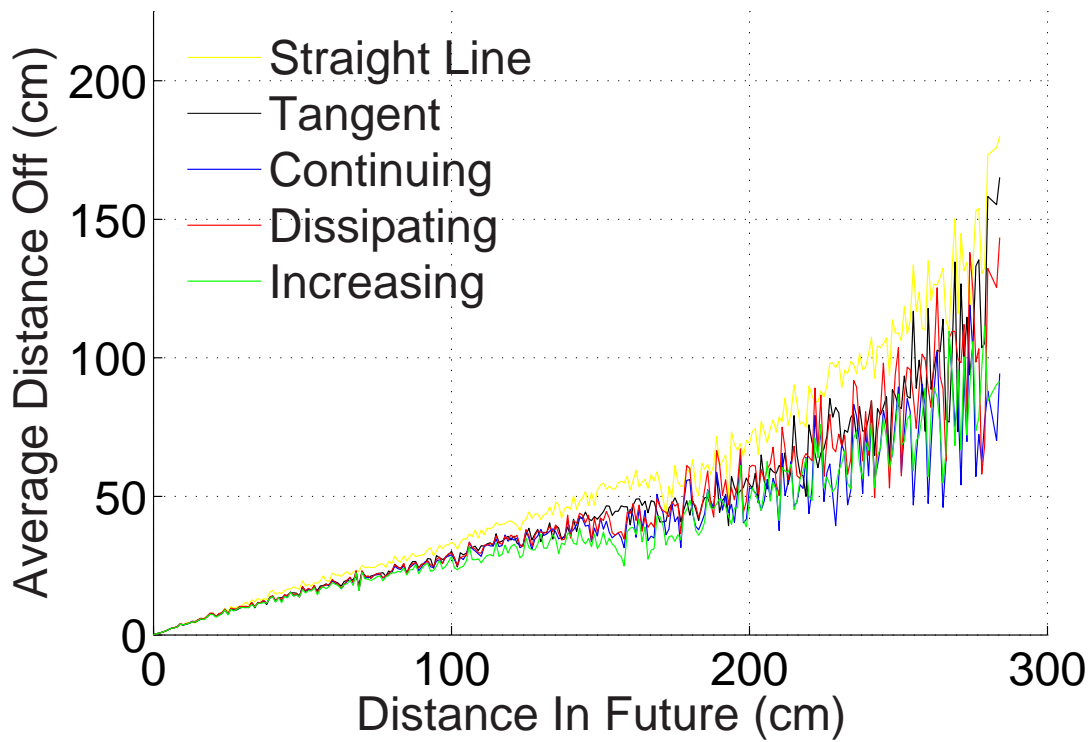


Figure A.4: Entire average distance from curve by distance graph for room entering data.

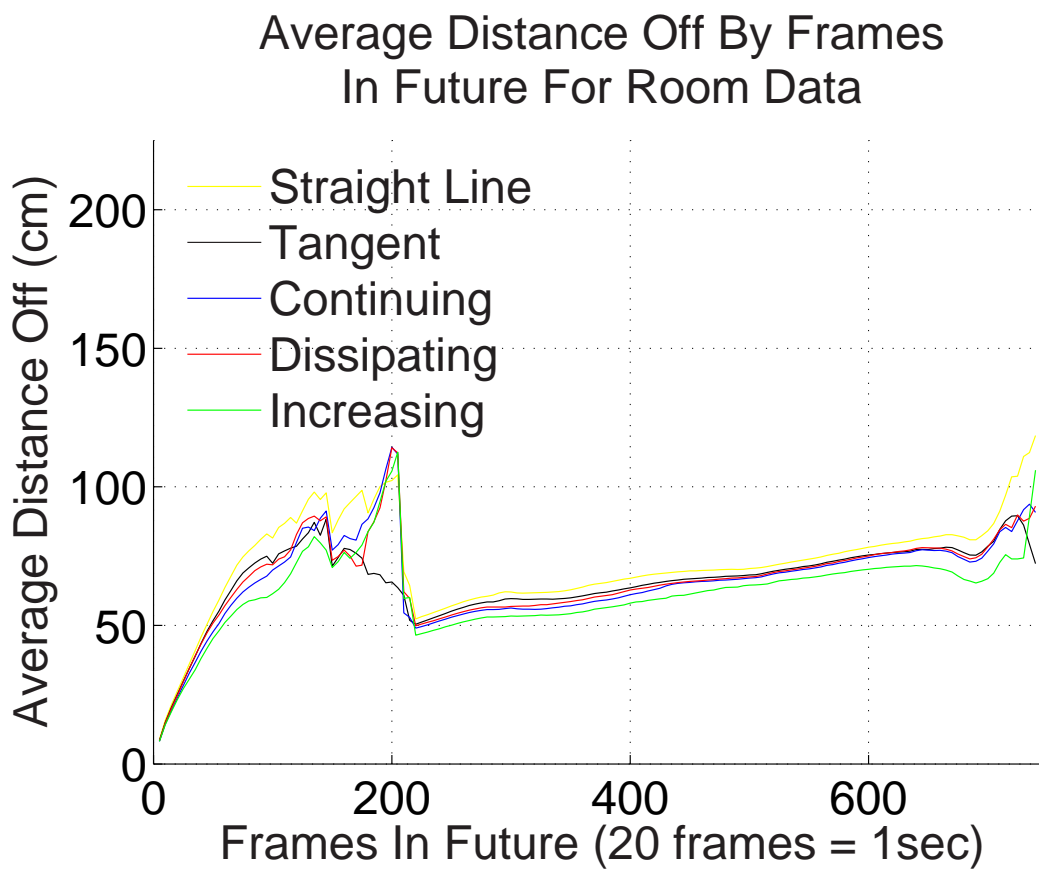


Figure A.5: Entire average distance from curve by frames graph for room data.

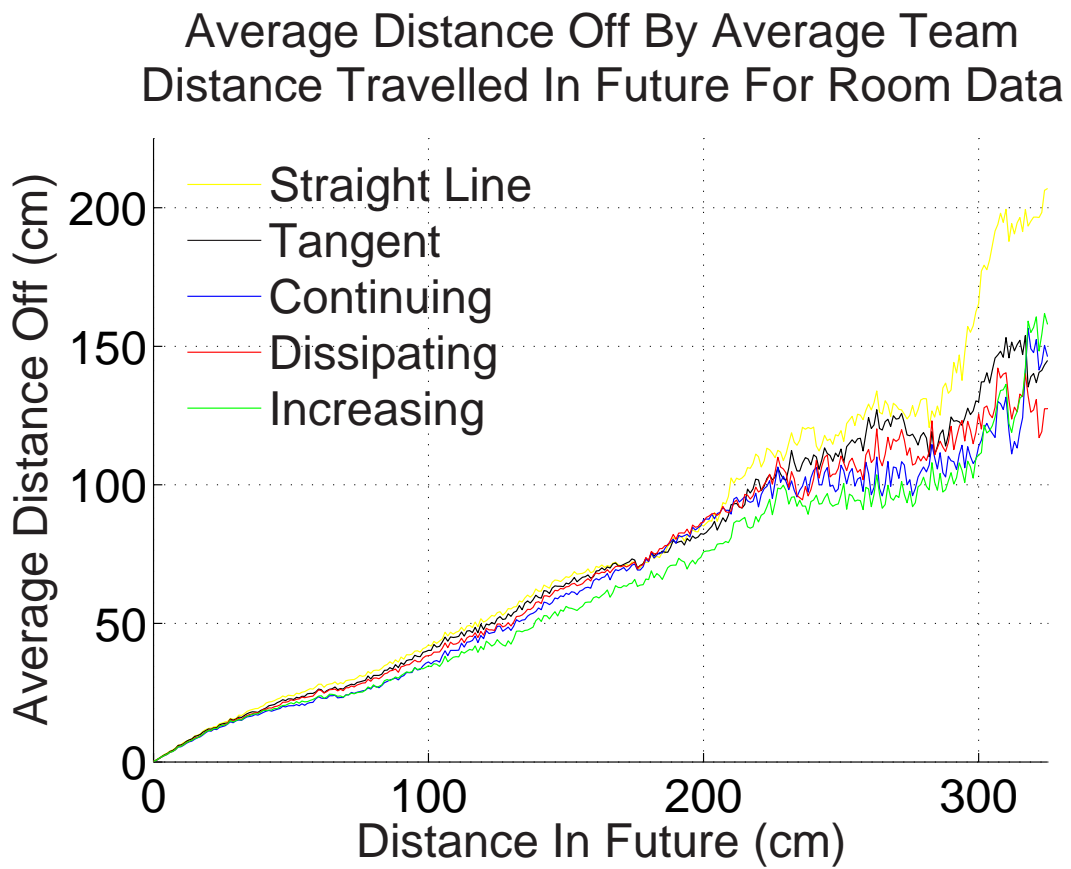


Figure A.6: Entire average distance from curve by distance graph for room data.